Central role of the p53 pathway in the noncoding-RNA response to oxidative stress

Paola Fuschi[1], Matteo Carrara[1], Christine Voellenkle[1], Jose Manuel Garcia-Manteiga[2], Paolo Righini[3], Biagina Maimone[1], Elena Sangalli[4], Francesco Villa[4], Claudia Specchia[4,5], Mario Picozza[6], Giovanni Nano[3,7], Carlo Gaetano[8], Gaia Spinetti[4], Annibale A. Puca[4,9], Alessandra Magenta[6], Fabio Martelli[1]

[1]Molecular Cardiology Laboratory, IRCCS Policlinico S. Donato, 20097, San Donato Milanese, Milan, Italy
[2]Center for Translational Genomics and BioInformatics, IRCCS San Raffaele Scientific Institute, 20132, Milan, Italy
[3]Operative Unit of Vascular Surgery I, IRCCS Policlinico S. Donato, 20097, San Donato Milanese, Milan, Italy
[4]Cardiovascular Research Unit, IRCCS MultiMedica, 20138, Milan, Italy
[5]Department of Molecular and Traslational Medicine, University of Brescia, Brescia, 25123, Italy
[6]Vascular Pathology Laboratory, Istituto Dermopatico dell'Immacolata-IRCCS, FLMM, Rome, Italy
[7]University of Milan, 20133, Milan, Italy
[8]Division of Cardiovascular Epigenetics, Department of Cardiology, Goethe University, Frankfurt am Main, 60596, Germany
[9]Department of Medicine and Surgery, University of Salerno, 84084, Salerno, Italy

Correspondence to: Fabio Martelli; email: fabio.martelli@grupposandonato.it
Keywords: oxidative stress, long noncoding RNAs, microRNAs, p53, endothelium
Received: October 12, 2017   Accepted: December 1, 2017   Published: December 12, 2017

ABSTRACT

Oxidative stress plays a fundamental role in many conditions. Specifically, redox imbalance inhibits endothelial cell (EC) growth, inducing cell death and senescence. We used global transcriptome profiling to investigate the involvement of noncoding-RNAs in these phenotypes. By RNA-sequencing, transcriptome changes were analyzed in human ECs exposed to H_2O_2, highlighting a pivotal role of p53-signaling. Bioinformatic analysis and validation in p53-silenced ECs, identified several p53-targets among both mRNAs and long noncoding-RNAs (lncRNAs), including MALAT1 and NEAT1. Among microRNAs (miRNAs), miR-192-5p was the most induced by H_2O_2 treatment, in a p53-dependent manner. Down-modulated mRNA-targets of miR-192-5p were involved in cell cycle, DNA repair and stress response. Accordingly, miR-192-5p overexpression significantly decreased EC proliferation, inducing cell death. A central role of the p53-pathway was also confirmed by the analysis of differential exon usage: Upon H_2O_2 treatment, the expression of p53-dependent 5'-isoforms of MDM2 and PVT1 increased selectively. The transcriptomic alterations identified in H_2O_2-treated ECs were also observed in other physiological and pathological conditions where redox control plays a fundamental role, such as ECs undergoing replicative senescence, skeletal muscles of critical limb-ischemia patients and the peripheral-blood mononuclear cells of long-living individuals. Collectively, these findings indicate a prominent role of noncoding-RNAs in oxidative stress response.

INTRODUCTION

Redox homeostasis plays a fundamental role in endothelial cell (EC) function and its imbalance elicits oxidative stress that has a causative role in many vascular diseases [1, 2]. Augmented EC oxidative stress is a result of increased production of reactive oxygen species from intracellular enzymes such as NADPH oxidase and uncoupled eNOS, as well as from mito-chondrial respiration, in the absence of counter-acting antioxidant defenses. As redox imbalance poses a major threat to EC function and survival, it triggers specific transcriptional and post-transcriptional modulation of gene expression [3, 4].

Aberrant control of gene expression underpins most pathologies. Thus, it is of pivotal importance to investigate how gene expression is regulated by the underlying factors of diseases, starting from oxidative stress.

Several hubs of cell response to oxidative stress have been identified, such as NRF2 and FOXO1, that increase the antioxidant defenses, and NFkB, that induces the transcription of pro-inflammatory cytokines [3, 4]. Another pivotal player is p53: it is activated by a multitude of stress stimuli, including reactive oxygen species, and, in turn, orchestrates an extremely complex anti-proliferative and pro-apoptotic transcriptional program [5].

Investigating the responses triggered by cell exposure to a single oxidative stress stimulus, such as a H_2O_2 bolus, might be instrumental to the identification of the molecular mechanisms underpinning more complex situations characterized by redox imbalance, such as proliferative senescence [6-8], limb ischemia [9-11] and aging [12, 13].

While the role of protein-coding transcripts in cell response to oxidative stress has been extensively studied [3, 4, 14], the importance of non-protein-coding RNAs (ncRNAs) has started to emerge only recently [9, 15].

ncRNAs are extremely heterogeneous [16]. Some RNAs, mostly with housekeeping functions, have been long known, such as ribosomal RNAs, transfer RNAs, as well as small nuclear and nucleolar RNAs. However, increasing attention has been dedicated in the last few years to two classes of regulatory ncRNAs: microRNAs (miRNAs) and long ncRNAs (lncRNAs).

miRNA are single-stranded, about 22 nt RNAs that regulate gene expression mostly by forming partial hybrids with target mRNAs and, in this manner, lowering their stability and/or translation efficiency [17]. Profiling of miRNA expression in H_2O_2-treated EC identified miR-200c as upregulated by oxidative stress. miR-200c induces EC apoptosis and senescence *via* ZEB1 inhibition and by disrupting the regulatory loop among SIRT1, FOXO1, and eNOS [18, 19].

LncRNAs are >200 nt long RNAs that are very heterogeneous both for their genomic organization and for their molecular mechanism of action [20]. They can be natural antisense (AS) expressed from the opposite strand of mRNAs, generated by intergenic regions (lincRNAs), localized in introns of annotated genes and transcribed from enhancers regulatory elements (eRNAs). Mechanistically, they can regulate gene expression epigenetically or acting as scaffolds for transcriptional repressors and activators. Certain lncRNAs can play a role in nuclear body compart-mentalization. Other lncRNAs regulate gene expression post-transcriptionally, modulating mRNA splicing and stability with different mechanisms. While lncRNAs are often expressed at low levels, some of them are sufficiently abundant to act as decoys for microRNAs (competing endogenous RNAs) and possibly other regulatory molecules.

LncRNAs regulate a variety of cell functions that might impact upon cell response to oxidative stress [15, 20]. In this study, we attempted to identify the involvement of lncRNAs and miRNAs in the molecular mechanisms underpinning EC response to oxidative stress. We profiled the transcriptomic changes induced by H_2O_2 treatment in EC, and validated the identified players and pathways with molecular and functional experiments. We also extended our investigation to other physio-logical and pathological conditions where redox imbalance plays a prominent role, suggesting that the ncRNAs identified might play a broader role in oxidative stress response.

RESULTS

H_2O_2 treatment inhibits endothelial cell growth

To analyze the transcriptomic changes induced by EC exposure to oxidative stress, human umbilical cord EC (HUVEC) were cultured in the presence or absence of 200 μM H_2O_2 for 16 hrs or 36 hrs, and total RNA was extracted. Cells derived from three different batches of HUVEC were used, in order to minimize the identification of transcriptomic responses characteristic only of specific EC isolates. To control the efficacy of the H_2O_2 treatment, HUVEC plates grown in parallel were assayed. Cell cycle profile analysis and bromo-deoxyuridine (BrdU) incorporation assay by FACS showed that, in the adopted condition, H_2O_2 treatment strongly decreased EC proliferation (Fig. S1A and B). The percentage of sub-G1 dead cells remained below 3% following H_2O_2 treatment, indicating a mostly

cytostatic response (Fig. S1A and C). HUVEC treated with solvent alone for 16 hrs were chosen as control to avoid the possibly confounding effects of cell confluency observed at 36 hrs. As further control, the ex-

pression of known H_2O_2 responsive genes was tested in the isolated RNAs by qPCR. As expected [9, 15], CDKN1A and miR-200c-3p expression were increased, while ZEB1 levels were reduced (Fig. S2).
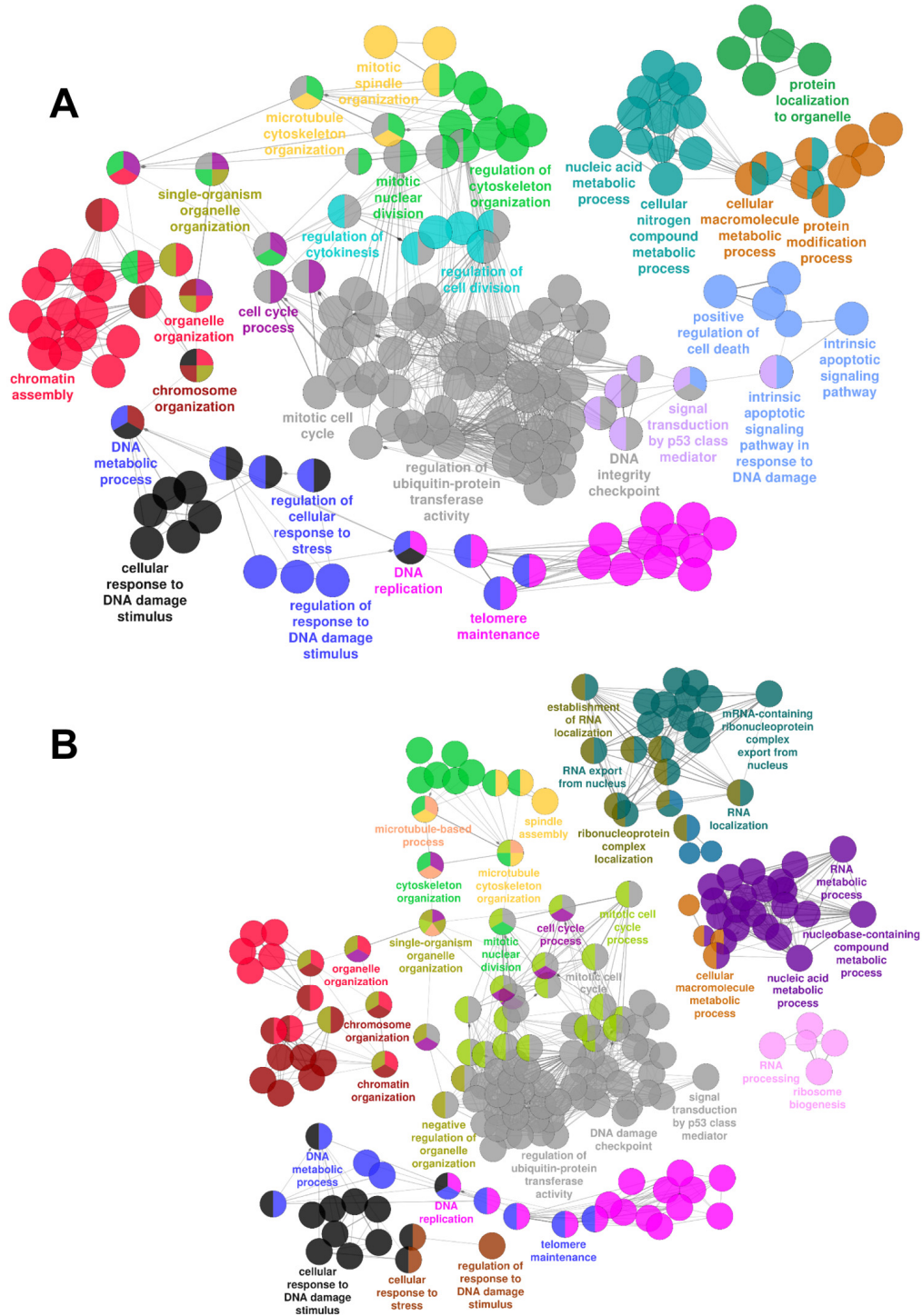

Figure 1. mRNAs differentially expressed upon HUVEC exposure to H_2O_2. Gene Ontology enrichment analysis of the transcriptomic changes induced by HUVEC treatment with H_2O_2 as assessed by rRNA-depleted RNA-sequencing. Circles represent specific ontology terms or KEGG pathways that were significantly enriched in the list of differentially expressed genes after 16 hrs (**A**) or 36 hrs (**B**) of H_2O_2 treatment (n= 3). Edges represent term connections within the ontology tree and colors highlight terms correlated in meaning. Terms are captioned if they are the most significant of the group or if they show a biological meaning connected to the system under analysis.

To analyze global changes in the transcriptome, mRNAs, lncRNAs and miRNAs profiles were measured by RNA-sequencing.

mRNA changes induced by H_2O_2 treatment indicate p53-pathway relevance

A total of 9 barcoded cDNA libraries were prepared from rRNA-depleted RNA derived from HUVEC cells exposed to H_2O_2 for 16 and 36 hrs or to solvent alone for 16 hrs. Reads were generated by next-generation sequencing yielding ≈ 1 billion forward and reverse reads after filters for quality and unique alignment to the human hg19 reference genome were applied.

Gene level analysis provided a total of ≈ 15 000 expressed genes and 76% of them were annotated as protein coding. Of these, ≈ 2 300 were significantly differentially expressed at 16 hrs (Dataset S1) and ≈ 3 100 at 36 hrs (Dataset S2); about 1800 genes were in common between the two timepoints (Dataset S3). These data indicate a profound effect of oxidative stress on HUVEC gene expression.

As expected, genes previously described as modulated by oxidative stress, such as CDKN1A, HMOX1, MCM6, GADD45A, and FAS [15] were among the most significantly modulated. This analysis was further validated measuring a subset of mRNAs by qPCR in independent samples of H_2O_2 treated HUVEC (Fig. S3).

In order to identify relevant biological functions, enriched biological processes and pathways were identified by ClueGO [21]. Gene ontology enrichment analysis at both 16 hrs (Fig. 1A) and 36 hrs (Fig. 1B) shows an enrichment in terms related to cell cycle, mitotic spindle/microtubules, DNA damage/stress response, apoptosis, chromatin and telomere integrity, RNA and nucleic acid metabolism, as well as p53 signaling.

Among the top modulated genes, both at 16 hrs and at 36 hrs, it was identified MDM2, a crucial negative regulator of p53, as well as a p53-induced gene [22]. A variety of MDM2 transcripts have been described [23]. Specifically, the expression of MDM2 transcripts with short 5'UTRs, including exon 1b, has been shown to be largely p53-dependent, unlike that of MDM2 isoforms with long 5'UTR, using exon 1a [23] (Fig. 2A). Of note, short 5'UTRs isoforms are more efficiently translated, establishing a p53/MDM2 negative feed-back loop [23, 24]. Differential exon usage analysis (Fig. S4) and qPCR validation (Fig. 2B), showed that, upon H_2O_2 treatment, MDM2 transcripts including exon 1b accumulated significantly, while transcripts including exon 1a did not (Fig. 2B).
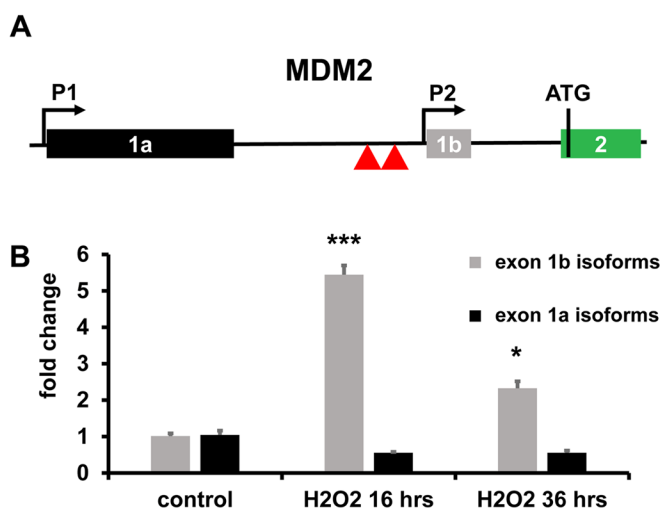
Figure 2. Differential MDM2 exon usage. (**A**) Genomic structure of the human MDM2 promoter region. The locus has two independent promoters before exons 1a (P1) and 1b (P2), yielding long- and short-5' UTR isoforms, respectively. Translation start site (ATG) in exon 2 is indicated. Red triangles indicate p53 protein binding sites involved in P2 activation. (**B**) In H_2O_2 treated HUVEC, short-5' UTR isoforms of MDM2 were induced, as assessed by qPCR using primers spanning from exon 1b to exon 2. Modulation of long-5' UTR isoforms of MDM2 was not statistically significant, as assessed by qPCR using primers spanning from exon 1a to exon 2. The bar graph represents average values ±SEM (n= 3; *p<0.05, ***p<0.001).

LncRNA modulations induced by oxidative stress

Gene expression analysis identified ≈ 1 000 lncRNAs, most lacking basic functional annotation. Of these, 101 and 208 were differentially expressed significantly at 16 hrs (Fig. 3A and Dataset S1) and at 36 hrs (Fig. 3B and Dataset S2), respectively, with 72 lncRNAs in common between the two timepoints (Dataset S4). Thus, data indicated a strong effect of oxidative stress on the expression also of ncRNAs in HUVEC. This analysis was validated measuring a subset of lncRNAs by qPCR in independent samples of H_2O_2-treated HUVEC. The heatmap in Fig. 3C shows side by side rRNA-depleted RNA-sequencing and qPCR data expressed in a $\log_2$ scale. Data expressed in a linear scale are shown in Fig. S5.

PVT1 is a potential oncogene that has been implicated in a variety of cancers, participating in DNA re-arrangements, interacting with MYC and encoding miRNAs [25]. PVT1 undergoes extensive alternative splicing to produce a wide variety of mature transcripts. In particular, a difference in exon 1a/1b usage has been observed after treatment with p53-inducing agents in cancer cells [26]. Likewise, in HUVEC, H_2O_2 treatment

led to a significant increase of p53-dependent exon 1b, while exon1a induction did not reach statistical significance (Fig. S6).
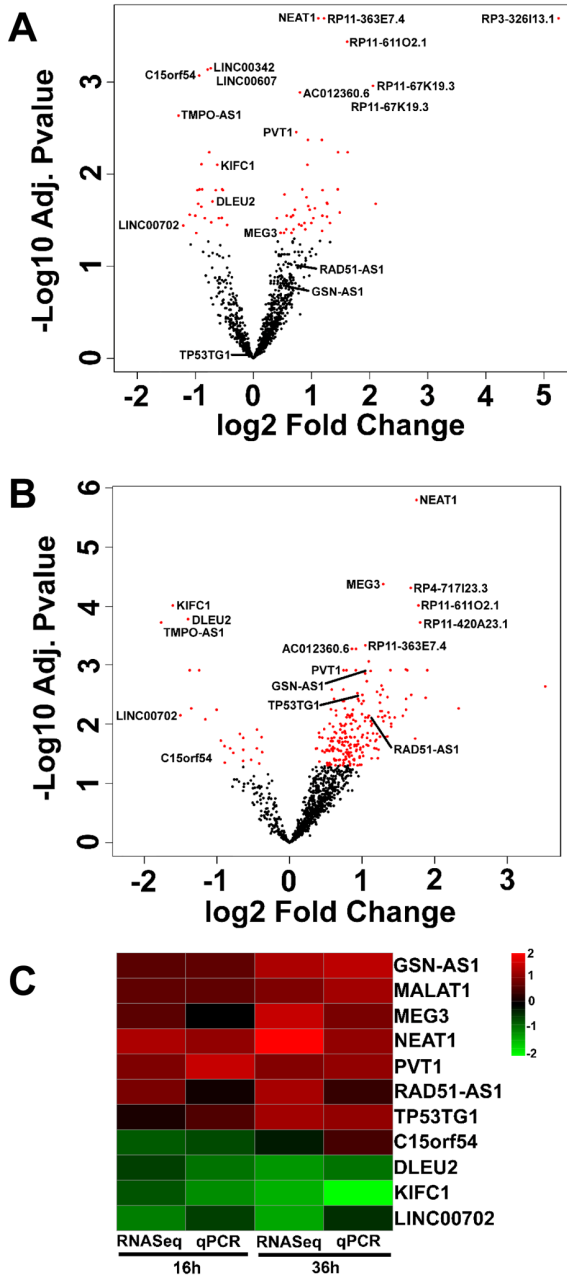

Figure 3. LncRNAs differentially expressed upon HUVEC exposure to H₂O₂. HUVEC were exposed to H_2O_2 for 16 hrs (**A**) and 36 hrs (**B**) and lncRNA expression was measured by rRNA-depleted RNA-sequencing (n= 3). Volcano plots show adjusted p values in a negative Log_{10} scale and fold changes in a log_2 scale. LncRNAs significantly (adjusted p values <0.05) modulated by H_2O_2 treatment are indicated in red. The names of top 10 modulated lncRNAs and of qPCR validated lncRNAs are indicated. (**C**) In independent HUVEC cultures treated as in **A** and **B** (n= 3), the modulation of the indicated lncRNAs was assayed by qPCR. The heat map shows modulated lncRNAs as log_2 values. Green= down-modulation; red= up-regulation.

miRNA/target interactions identify miR-192-5p as a hub of endothelial cell response to H₂O₂

To analyze miRNA expression changes induced by EC exposure to oxidative stress, RNAs derived from HUVEC treated with H_2O_2 for 16 hrs were analyzed by small RNA-sequencing.

After trimming filters for quality and unique alignment to the human hg19 reference genome were applied, ≈ 7.5 million reads were obtained allowing the detection of ≈ 100 miRNAs (DataSet S5). Among miRNAs that escaped detection there were miR-200-family members. Differential expression analysis identified 9 significantly modulated miRNAs (DataSet S5). Quite surprisingly, miR-16 appeared to be modulated by H_2O_2, in disagreement with previous findings [9, 18]. qPCR validation on RNAs derived from independent experiments showed that indeed miR-16 was not modulated by H_2O_2. Conversely, miR-192-5p, miR-30a-5p, miR-381-3p, miR-769-5p and let7i-5p were significantly up-regulated, both at 16 and 36 hrs of H_2O_2 treatment (Fig. 4A and supplementary Fig. S7 in linear scale). Bioinformatic analysis using miRTarBase [27] and Cytoscape [28] highlighted interactions between validated miRNAs and reciprocally modulated genes that had been identified as targets of these miRNAs. Fig. 4B identified miR-192-5p as a hub of miRNA/target interactions in EC response to H_2O_2. Accordingly, gene ontology analysis of potential miR-192-5p targets displayed an enrichment in terms related to cell cycle, DNA damage/stress response and microtubules (Fig. 4C).

Next, we investigated whether miR-192-5p induction could be prevented by reactive oxygen species scavengers. To this aim, we treated HUVEC with the alkylating agent 1,3-bis(2 chloroethyl)-1-nitrosourea (BCNU), an inhibitor of glutathione reductase that blocks the conversion of oxidized to reduced glutathione [29], in the presence or absence of N-acetyl-L-cysteine (NAC) to prevent the decrease in intracellular reduced glutathione induced by BCNU [29]. Incubation of HUVEC with 0.25 mM BCNU for 2 h increased miR-192-5p levels and this phenomenon was inhibited by preincubation with 10 mM NAC (Fig. S8).

To further validate the relevance of miR-192-5p role in EC growth, we tested the effect of miR-192-5p overexpression in the absence of oxidative stress. miR-192-5p expression decreased the mRNA levels of two predicted targets, TMPO and CDC25A (Fig. 5A), that were also down-modulated in H_2O_2 treated cells (Dataset S3). miR-192-5p expression has been shown to activate p53 pathway in cancer cells [30-33]. Likewise, its expression in HUVEC induced the expression of the p53

targets CDKN1A, FAS and GADD45A (Fig. 5A), that were also increased in H_2O_2 treated cells (Dataset S3). In keeping with these findings, miR-192-5p dramatically decreased HUVEC growth, inducing cell death (Fig. 5B).
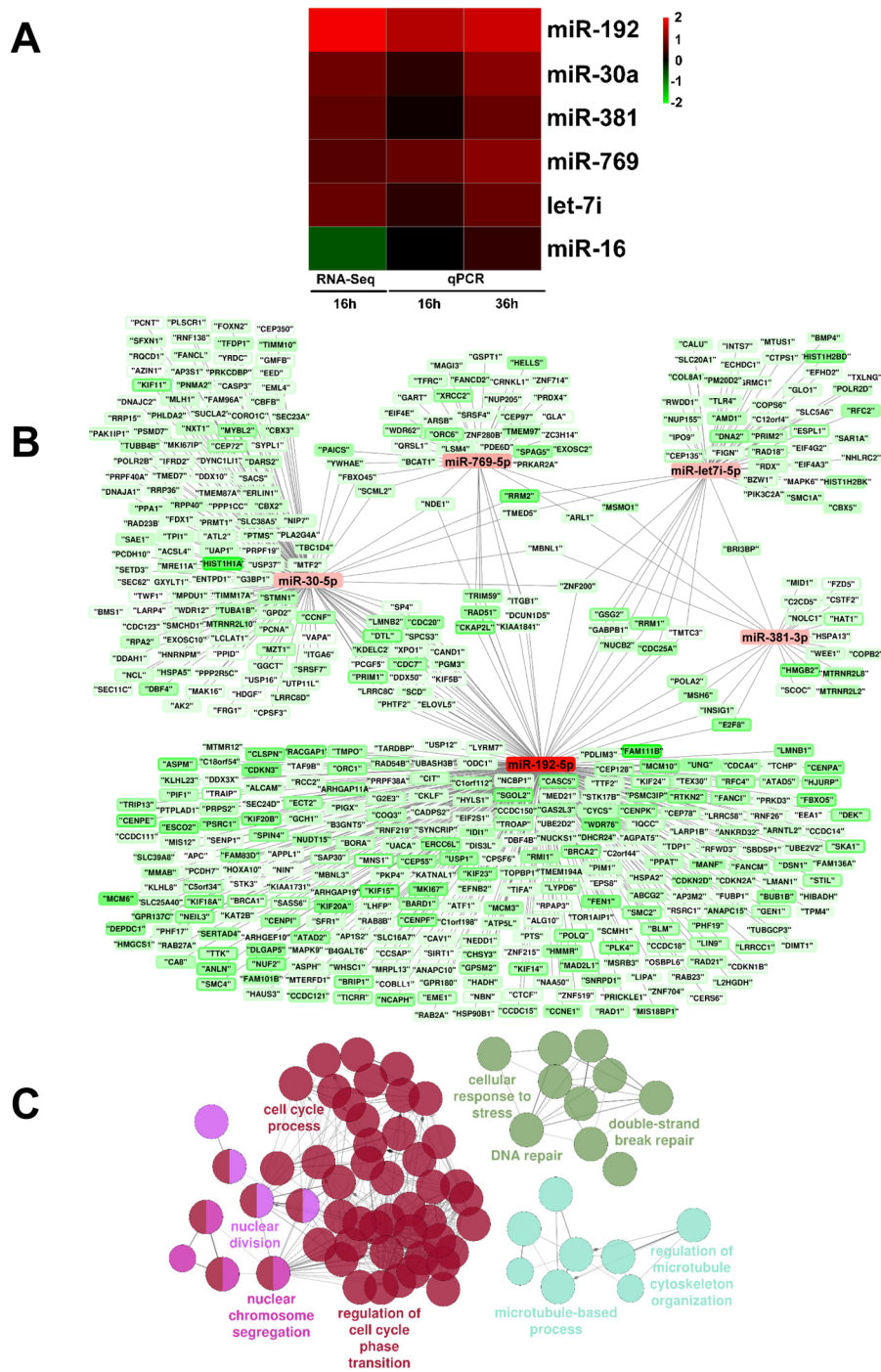

Figure 4. miRNAs differentially expressed upon HUVEC exposure to H_2O_2. (**A**) HUVEC were exposed to H_2O_2 for 16 hrs and miRNA expression was measured by small RNA-sequencing (n= 3). Validation was performed by qPCR in independent HUVEC cultures treated with H_2O_2 for 16 hrs and 36 hrs (n= 3). The heat map shows modulated lncRNAs as log_2 values. Green= down-modulation; red= up-regulation. (**B**) Interactions between qPCR-validated miRNAs and their potential targets, as reported by miRTarBase, that showed a significant down-regulation at both 16 hrs and 36 hrs time points in rRNA-depleted RNA-sequencing data. Results were represented using Cytoscape: For each gene, the inner color represents the log_2 fold change at 16 hrs and the border color represents the log_2 fold change at 36h. (**C**) miR-192-5p targets enrichment analysis. Enrichment analysis performed with ClueGO on miR-192-5p targets that showed a significant down regulation at both time points in rRNA-depleted RNA-sequencing data. Circles represent specific ontology terms or KEGG pathways that are significantly enriched. Edges represent terms connections within the ontology tree and colors highlight terms correlated in meaning. Terms are captioned if they are the most significant of the group or if they show a biological meaning connected to the system under analysis.
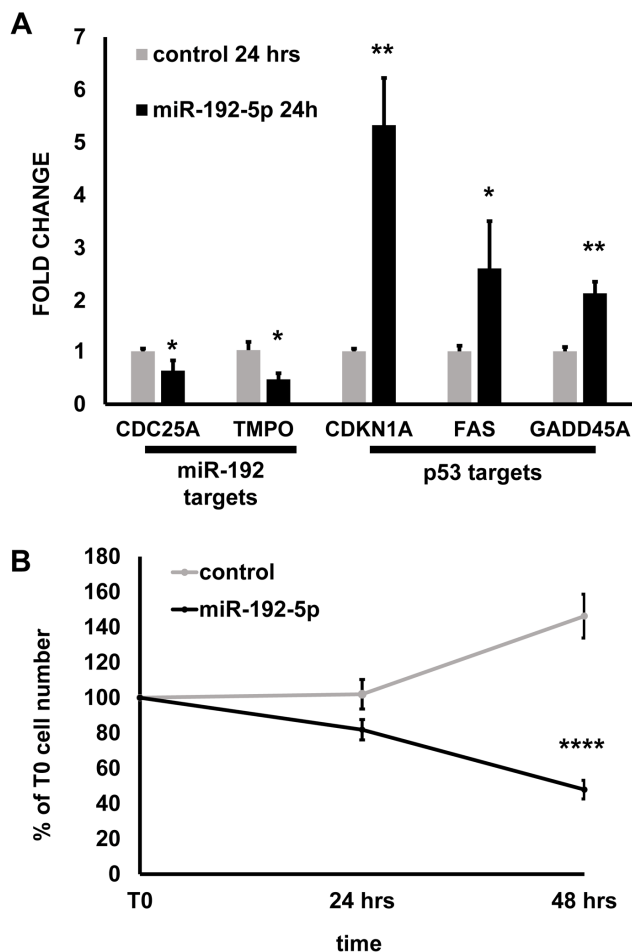
A

B

Figure 5. miR-192-5p overexpression inhibits EC growth. HUVEC were transfected with miR-192-5p mimic or control oligonucleotides. The next day, cells were plated at 200 000 cells/p3 plate density (T0) and harvested 24 and 48 hrs later. (**A**) The expression of the indicated genes was measured by qPCR at 24 hrs from T0. The bar graph represents average values ±SEM (n= 3; *p<0.05 **p<0.01). (**B**) Cells were counted at 24 hrs and 48 hrs from plating (T0) and plotted as % of the T0 cell number. miR192-5p expression inhibited HUVEC growth significantly. The graph represents average values ±SEM (n=8 independent transfections; **** p<0.0001).

p53 implication in the regulation of noncoding RNAs by H_2O_2

Given the importance of p53 for mRNA modulation by oxidative stress highlighted by the gene ontology analysis (Fig. 1), we investigated whether the same was true for lncRNAs.

In order to identify p53 binding sites in the regulatory regions of the identified H_2O_2-modulated lncRNAs, we took advantage of a publicly available ChIP-sequencing (ChIP-seq) datasets for p53.

Since no p53 ChIP-seq datasets have been published so far in ECs, we used data derived from osteosarcoma cells treated with nutilin, an activator of p53 [34]. The region encompassing 5 kbp upstream and 2 kbp downstream the transcription start site of each lncRNA was analyzed for the presence of significant (False Discovery Rate, FDR,< 0.001) peaks corresponding to a consensus p53 binding-site. As expected, known p53 targets such as CDKN1A and GADD45A displayed very significant peaks (Fig. S9A and B). It was found that 29 lncRNAs modulated by H_2O_2 in HUVEC also displayed at least one significant peak for p53 protein in nutilin treated osteosarcoma cells (Supplementary Dataset S6 and Fig. S9C, D and E). Patterns of alternative exon usage for PVT1 and MDM2 were observed as well (Fig. S9E and F). This analysis strongly suggests that p53 might regulate the identified lncRNAs in H_2O_2 treated ECs.

To corroborate this hypothesis, modulation by oxidative stress of a subset of target genes was analyzed by qPCR in HUVEC where p53 had been knocked down. HUVEC transfection with p53 siRNAs significantly decreased the corresponding transcript (Fig. 6A). As expected, the mRNA levels of known p53 targets, such as CDKN1A and FAS1, were significantly decreased by p53 silencing, both in the presence or absence of H_2O_2 treatment (Fig. 6A). Likewise, induction by H_2O_2 of exon-1b containing transcripts of MDM2 was also blocked (Fig. 6A). When ncRNAs were analyzed, it was found that p53 knock-down significantly inhibited the induction of predicted p53 target lncRNAs MALAT, NEAT and PVT1 upon H_2O_2 treatment (Fig. 6B). miR-192-5p has been described to be a p53 transcriptional target in a variety of cancer cells [30-32]. However, miR-192-5p precursor transcripts were undetectable by small RNA-sequencing in HUVEC, escaping our analysis. Thus, we measured by qPCR whether the levels of mature miR-192-5p were affected by p53 silencing. Fig. 6B shows that, indeed, p53 knock-down prevented miR-192-5p induction in H_2O_2-treated HUVEC.

Noncoding RNA modulation in senescent endothelial cells

Next we wanted to assess whether the ncRNA alterations identified in H_2O_2-treated HUVEC were present also in other experimental systems characterized by altered redox balance. Specifically, replicative senescence is closely interlinked with increased oxidative stress, and it is characterized by a strong activation of the p53 stress-response pathway [6-8]. As expected [11, 35], late passage HUVEC displayed senescence markers, such as increased CDKN1A and GADD45A mRNA levels, decreased RAD51 mRNA and were

mostly positive for senescence-associated β-galactosidase activity (Fig. S10). When a subset of H_2O_2-modulated lncRNAs and miRNA was assayed, they all displayed increased levels in late passage HUVEC (Fig. 7A). Moreover, both MDM2 and PVT1 exhibited a pattern of differential exon usage similar to that observed in response to H_2O_2 (Fig. 7B). Indeed, while exon 1a isoforms were not modulated, exon 1b isoforms of MDM2 and PVT1 were increased in senescent HUVEC.

miR-192-5p increase in ischemic muscles

Critical limb ischemia (CLI) is associated to increased oxidative stress levels in the ischemic muscles [9-11]. Thus, we investigated whether the ncRNA alterations

identified in H_2O_2-treated HUVEC were present also in this system. Ischemic muscles are characterized by necrosis and inflammation, often precluding the possibility to isolate high quality RNAs. Thus, our analysis was limited to miRNAs, that are more resistant to degradation [11, 36], and in particular to miR-192-5p, the most significantly modulated miRNA in H_2O_2 treated ECs. Skeletal muscle samples were harvested from the ischemic limb of patients undergoing amputations for CLI. Specifically, ischemic tibialis anterior muscles were compared to non-ischemic sartorious muscle samples harvested at the amputation site of the same patient. Figure 8 shows that miR-192-5p levels were significantly increased in ischemic muscles.

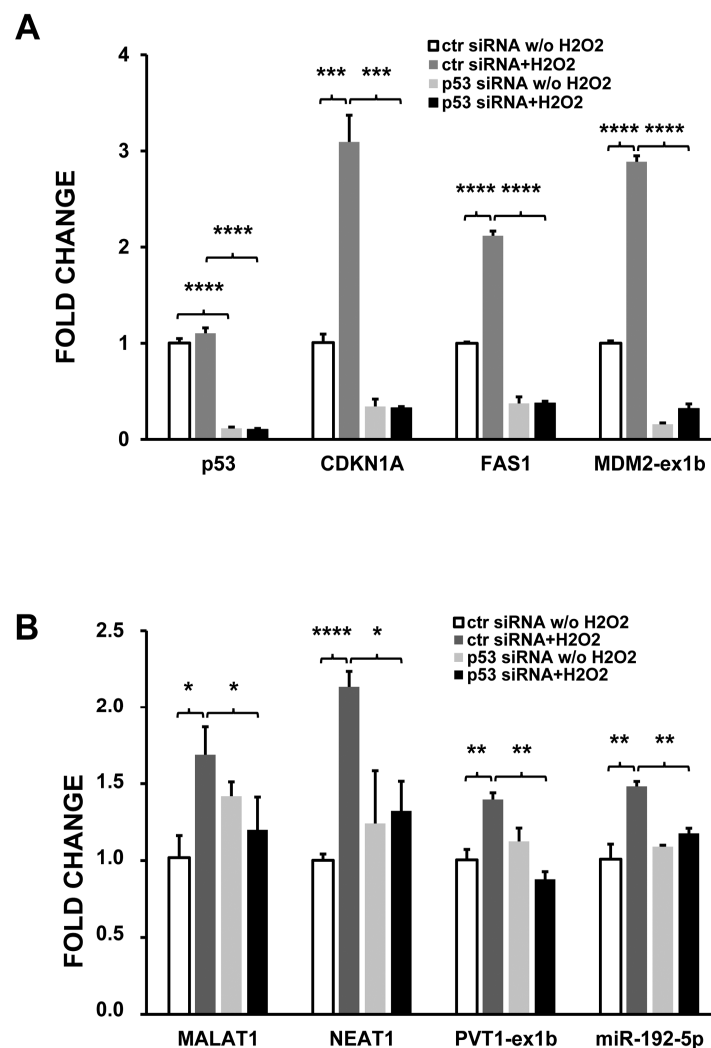miR-200c-3p was also tested, but was not detectable.

Figure 6. p53 silencing inhibits the induction of target ncRNAs by H_2O_2. HUVEC were transfected with p53 or control (ctr) siRNAs and, 24 hrs later, treated with either 200 μM H_2O_2 or solvent alone. After 16 hrs, total RNA was extracted and the indicated RNAs analyzed by qPCR. (**A**) coding RNAs; (**B**) ncRNAs. The bar graphs show average fold changes ±SEM of the indicated RNAs referred to untreated cells transfected with control siRNA (n= 3; *p<0.05,**p<0.01, ***p<0.001).

Altered levels of H₂O₂-response RNAs in the peripheral blood of long living individuals

Oxidative stress response pathway has been linked to aging [12, 13] and the fine regulation of the stress response is crucial for healthy aging [37]. Thus, we hypothesized that long-living individuals (LLIs) might have moderate oxidative stress levels and, as a consequence, low levels of stress-response genes. To test this hypothesis, we measured the levels of coding and noncoding H₂O₂-response RNAs in the peripheral blood mononuclear cells (PBMCs) of LLIs [38, 39]. Specifically, 53 LLIs (98.2±4.1 years old) were compared to 65 controls (49.2±14.2 years old). Results show a global reduction of H₂O₂-response RNAs in LLIs (Fig. 9), with the exception of MDM2 isoforms, MEG3 and miR-200c-3p (Fig. S11).

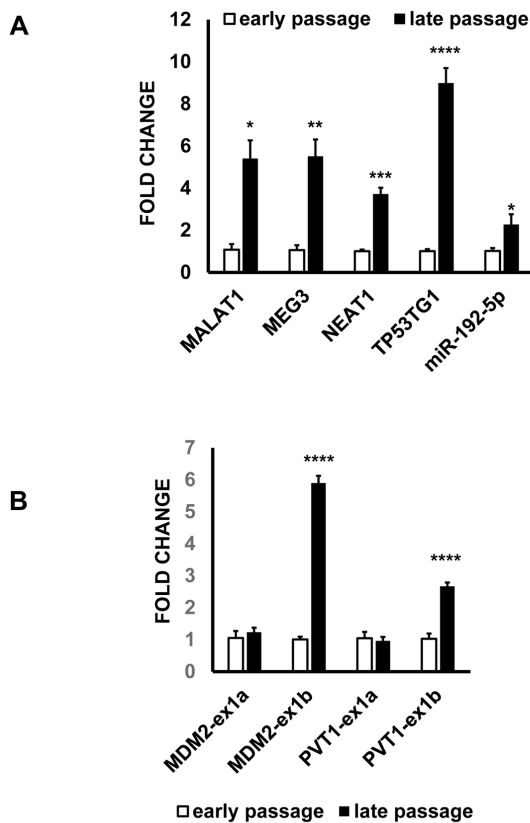Among the LLIs, 28 were frail (i.e. with age-associated disease) and frailty appears to be associated with higher oxidative stress levels [40]. Thus, significantly modulated RNA levels were compared between healthy and frail LLIs. It was found that H₂O₂-induced lncRNAs MALAT1 and NEAT1 levels were significantly lower in healthy LLIs (Fig. 10).
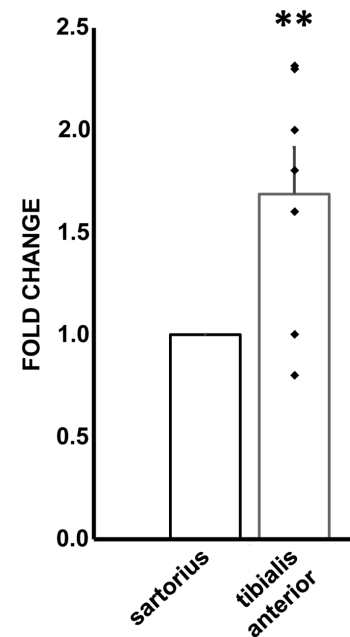

Figure 8. Increased miR-192-5p levels in ischemic muscles. Skeletal muscle samples were harvested from the ischemic limb of patients undergoing above the knee amputations for CLI. Tibialis anterior and sartorious muscle samples were harvested and total RNA was extracted. The bar graph shows average ±SEM miR-192-5p levels measured by qPCR. Values of individual patients are indicated as black squares. For each individual, ischemic sartorius muscle values are referred to non-ischemic sartorius values (n= 7; **p< 0.01).

Figure 7. ncRNA alterations identified in H₂O₂-treated ECs are also present in senescent HUVEC. Total RNA was extracted from early and late passage HUVEC and the indicated RNAs were tested by qPCR. The bar graphs represent average values ±SEM (early passage n= 3, late passage n= 7; *p<0.05, **p<0.01, ***p<0.001, ****p<0.0001). **(A)** ncRNAs. **(B)** Differential exon usage. Exon 1b isoforms of MDM2 and PVT1 are p53-regulated.

DISCUSSION

In the present study, the differential expression landscape of protein-coding and non-coding transcripts in H₂O₂ treated ECs was outlined by next-generation sequencing.

H₂O₂ concentration used in this study induced a strong cytostatic effect and very low EC death *in vitro*, in keeping with previous studies [18, 19, 41-48]. Therefore, the ensuing redox imbalance is likely close or below to levels expected to occur in many pathophysiological conditions, such as reperfusion injury, when oxidative stress can induce not only growth arrest but also extensive cell death [49-51]. It is worth noting that other ECs might be more sensitive to H₂O₂. For instance, Park reported that H₂O₂ inhibited the growth of Calf Pulmonary Artery Endothelial Cells (CPAECs)

and HUVECs at 24 h with IC50 of approximately 20 and 300 μM, respectively [52].

After filtering of rRNA-depleted RNA-sequencing datasets, we analyzed about 120 million of paired-end reads per sample, allowing the measurement of low expressed mRNAs and lncRNAs. Validation performed by qPCR on independent samples confirmed the accuracy of our analysis for all RNA species.

A recent study reported the transcriptome profiling of 3D co-cultured cardiomyocytes and human ECs under oxidative stress [53]. In the conditions adopted by the authors, a very limited number of genes was modulated in ECs, possibly due to the stabilizing action of the co-culture with cardiomyocytes.

Our analysis was also extended to miRNAs, facilitating the identification of miRNA/mRNAs interactions. Of
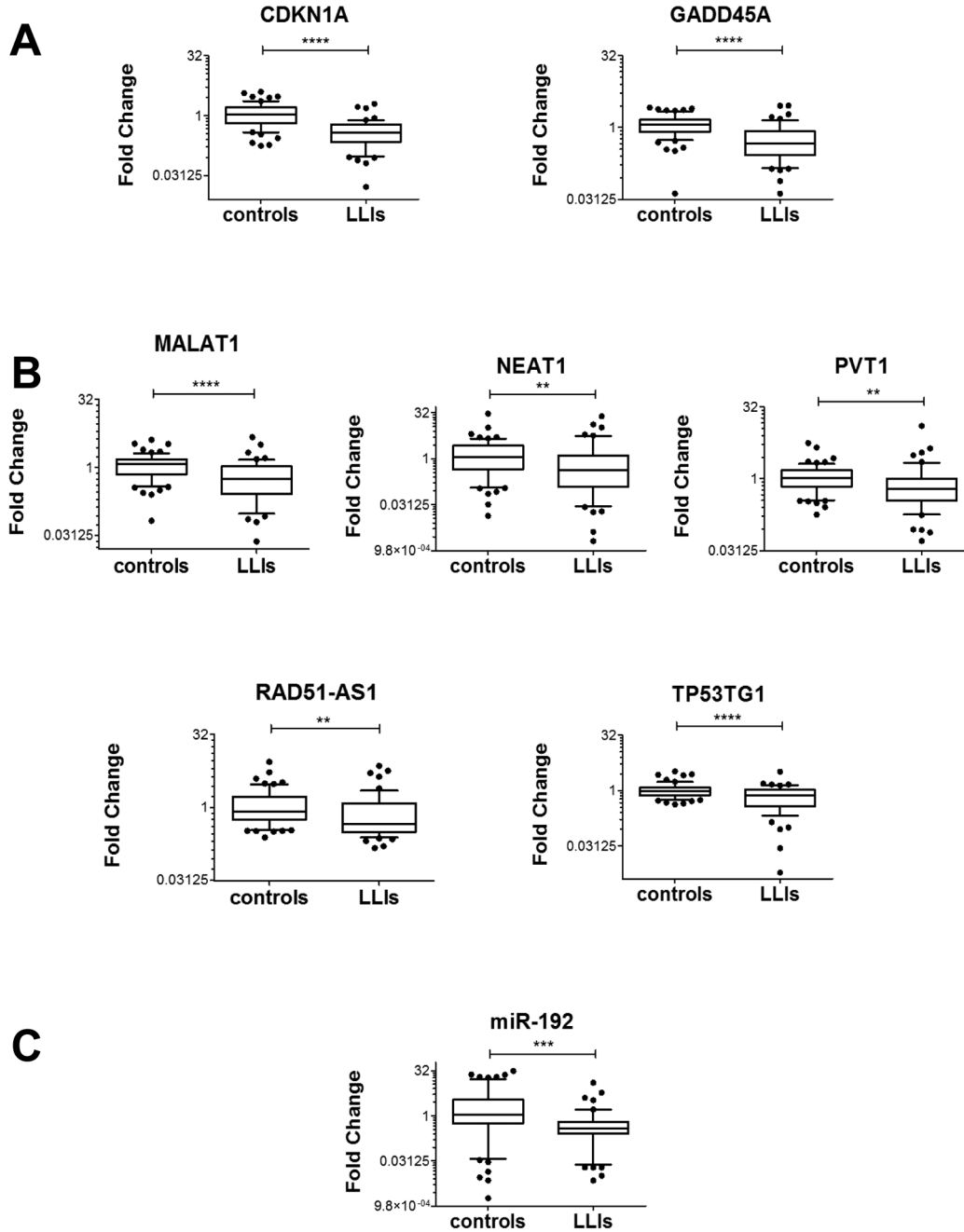

Figure 9. Association between H$_2$O$_2$-responsive RNA levels and life-span. Box plots of the indicated RNAs in LLIs (n= 53) versus controls (n= 65); (*p≤0.05, **p≤0.01, ***p<0.001, ****p<0.0001 after adjustment for sex distribution). (**A**) Coding RNAs. (**B**) LncRNAs. (**C**) miRNAs.
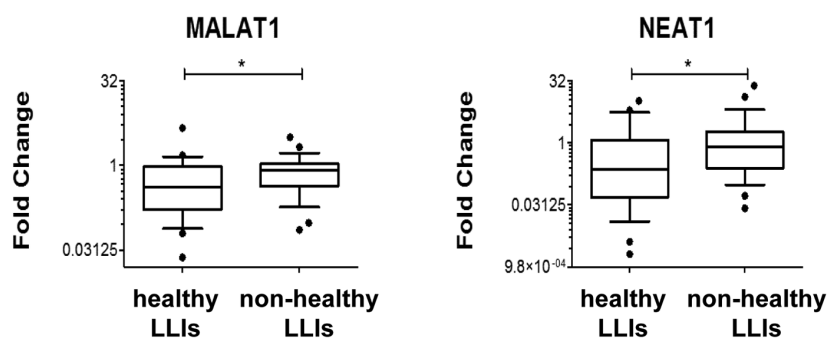
Figure 10. Association of MALAT1 and NEAT1 levels to healthy life-span. Box plots of the indicated RNAs in LLIs subdivided based on the presence/absence of age-associated diseases (healthy n= 25; non-healthy n= 28; *p<0.05 after adjustment for sex distribution).

note, results were not completely overlapping with a previous study performed by our group in H_2O_2-treated HUVEC, most likely due to differences in cell culture conditions and in profiling technologies, i.e. qPCR-arrays [19] *vs* next generation sequencing (this study). Indeed, miR-200c-3p and miR-1 found to be significantly modulated by qPCR-arrays [19], were not included in the small RNA-sequencing libraries, possibly also because very little expressed in ECs. On the other side, in the qPCR-array study [19] miR-192-5p was induced by H_2O_2 treatment, but not further pursued, miR-16-5p was not modulated, while probes for miR769-5p were not present in the array. Single miRNA qPCR assays for miR-200c-3p and miR16-5p fully reconciled the two investigations.

Data analysis showed a pivotal role of p53 [5] in EC response to oxidative stress and this pervasive p53 action was not limited to coding transcripts, but was extended to lncRNAs and miRNAs. Accordingly, many validated p53 target mRNAs were modulated and enriched biological processes and pathways included not only p53 signaling, but also many other related categories, such as cell cycle, DNA damage/stress response and apoptosis.

LncRNAs seem to be part of the p53-pathway as well. Indeed, among the H_2O_2-modulated lncRNAs in HUVEC, MEG3 has been found to be an activator of p53 in other systems [54, 55] and p53 induces formation of NEAT1-containing paraspeckles, that modulate replication stress response and chemosensitivity [56]. Moreover, MALAT1-depleted fibroblasts are sensitive to p53 levels, indicating that p53 is an effector of MALAT1 pro-proliferative activity [57].

Potential promoter analysis and survey of public p53 ChIP-seq datasets, indicated 29 lncRNAs modulated by

H_2O_2 in ECs as p53-target candidates. Accordingly, when a subset of them was assayed in p53-silenced HUVEC, their induction by H_2O_2 was blunted. These observations are also in keeping with data in other experimental systems: indeed, PVT1 [26], NEAT1 [58] and TP53TG1 [59] have been found to be p53 transcriptional targets in a variety of cancer cells. Another lncRNAs activated by HUVEC treatment with H_2O_2 in a p53-dependent manner was MALAT1. However, the role played by p53 might be context dependent. Indeed, in mouse erythroid myeloid lymphoid cells undergoing differentiation, p53 binds to Malat1 promoter repressing its transcription [60].

It is worth noting that *NEAT1* and *MALAT1* loci are adjacent to one another in the genome. Independent p53-binding sites were present upstream their transcription start sites, but it is tempting to speculate that they might be functionally related.

Another important noncoding player in p53 pathway seems to be miR-192-5p. Indeed, in keeping with previous observations in cancer cells [30-32], miR-192-5p activation was p53-dependent; its expression, in turn, increased the levels of p53-targets, leading to EC growth arrest and death. Accordingly, evidence of a p53-miR-192-5p positive feed-back loop has been found also in multiple myeloma as well as in colon, breast, lung and ovary cancer cell lines [30-33, 61]. Finally, a similar feed –forward mechanism has been identified by our group for p53 and miR-200-3p as well [18, 19].

Bioinformatic analysis of the interactions between the identified miRNAs and their modulated predicted targets, indicated miR-192-5p as a potential hub of the EC response to H_2O_2. Interestingly, gene ontology analysis of miR-192-5p targets identified p53-related

categories, such as cell cycle and DNA damage/stress response.

Library sequencing depth and the low expression levels of many transcripts precluded a high-throughput analysis of alternative exon usage events. Nevertheless we were able to show p53-dependent use of starting exons for both MDM2 [23] and PVT1 [26]. Exon 1b-containing isoforms of MDM2 mRNA are efficiently translated and their p53-driven transcription prompts p53/MDM2 negative feed-back loop [23, 24]. The functional consequences of PVT1 alternative 5' exons usage are not clear to date, but it it is possible to speculate that it might change the transcript secondary structure.

We also showed that the lncRNA and miRNA alterations identified in H_2O_2-treated HUVEC were present also in other experimental systems where redox balance alteration plays a significant functional role. In particular, replicative senescence is closely interlinked with increased oxidative stress, shares many molecular mechanisms with H_2O_2-induced senescence and it is characterized by a strong activation of the p53 stress-response pathway [6-8, 62]. Indeed, all of the lncRNAs, miRNAs and alternative exon usage events identified in H_2O_2-treated cells that we tested were observed also in senescent EC.

The molecular mechanisms identified in ECs cultured *in vitro* might be also important in physiological and pathological conditions in humans. CLI is associated to increased oxidative stress levels in the ischemic muscles and redox imbalance plays a causal role in ischemia-induced tissue damage [9-11, 63]. We found that miR-192-5p levels were increased in ischemic muscles of CLI affected patients. The anti-proliferative and pro-apoptotic activity of miR-192-5p relates with the poor regenerative and cell death milieu observed in the muscles of CLI patients [10]. Unfortunately, low patient numerosity precluded miR-192-5p correlation with clinically relevant parameters.

Another relevant condition is aging. The deterioration with age of the stress response mechanisms increases the risk of many age-related diseases. In contrast, LLIs display preserved stress response mechanisms, likely derived from a combination of a healthy lifestyle and a favorable genetic background. The integration of these factors could allow LLI to maintain moderate oxidative stress levels that exert beneficial signaling and modulatory effects on cellular metabolism [37].

Accordingly, we found that out of 12 coding- and noncoding-RNAs tested in PBMCs, most displayed decreased levels in LLIs compared to control individuals. While several interpretations are possible, the simplest explanation is that the moderate oxidative stress levels characterizing LLIs are associated to lower levels of RNA species involved in the cell response to redox imbalance. In this respect, the levels of MALAT1 and NEAT1 seem to be particularly informative, since they displayed decreased levels in healthy compared to frail LLIs, emerging as potential biomarkers of healthy aging.

While the functional interaction between MALAT1 and NEAT1 is still largely unknown, one might speculate that they might play separate, but complementary roles in cell response to stress. These abundant nuclear enriched transcripts share some features [15, 64] and are both hypoxia-induced [65, 66]. MALAT1 localizes to nuclear speckles, which are nuclear bodies enriched for serine and arginine-rich splicing factors. NEAT1 is required for the formation of a different type of nuclear bodies, named paraspeckles for their close proximity to speckles. Of note, paraspeckles have been implicated in sequestering RNAs that respond to cellular stress [15, 64]. Thus, low MALAT1 and NEAT1 in healthy LLIs likely correlates with reduced cellular stress.

NEAT1 and MALAT1 co-enrich a number of *trans* genomic binding sites and protein factors [67]. However, MALAT1 primarily localizes within gene bodies and near the transcriptional start-sites, while NEAT1 localizes preferentially to transcriptional start- and termination-sites, suggesting independent but complementary roles for these RNAs in regulating nuclear bodies organization [67].

In conclusion, a RNA-sequencing approach was used to identify protein-coding and non-coding RNAs modulated in human ECs exposed to H_2O_2. We showed that these findings were not limited to this specific setting but could be extended to other conditions, such as proliferative senescence, CLI and healthy aging. Thus, the present study may contribute further insight into the biological functions and molecular mechanisms of lncRNAs and miRNAs in physiological and pathological conditions where redox imbalance plays a causal role.

MATERIALS AND METHODS

Cell cultures and transfections

HUVEC (Clonetics for profiling experiments or Thermo Fisher for all the other experiments) passage ≤4 were cultured in EGM-2 (Cambrex) at 37°C in a humidified atmosphere of 5% CO_2- 95% air. N-acetyl-L-cysteine (NAC, Sigma) and 1,3-bis(2 chloroethyl)-1-nitrosourea (BCNU, Sigma) were dissolved in water.

HUVEC were transfected with 60 picomoles of a mix of TP53HSS110905/TP53HSS186391/TP53HSS186390 Stealth p53-RNAi, with 50 picomoles of hsa-miR-192-5p mirVana miRNA mimic (Life Technologies) or with negative control #1 (Life Technologies) using siRNA transfection reagent (Santa Cruz Biotechnology) in 40% confluent HUVECs, according to the manufacturer's manual. When relevant, cells were exposed to 200 μM H_2O_2 24 hrs after transfection.

In replicative senescence experiments, early and late passage HUVEC underwent 8 and 18 population doublings, respectively. Population doublings were calculated as described previously [68]; briefly, the number of population doublings that occurred between passages was calculated according to the following equation: population doublings = $\log_2(Ch/Cs)$, where Ch is the number of viable cells at harvest and Cs is the number of cells seeded.

Flow cytometry

HUVEC were incubated for 30 min with 20 μM BrdU (Sigma) and then fixed with 70% ethanol. Cell cycle analysis was performed by combined anti-BrdU (Becton Dickinson) and propidium iodide (PI) staining using a Becton Dickinson flow cytometer. Cell Quest software was used to determine the percentage of BrdU-positive cells.

Library preparation and RNA-sequencing

Total RNA was extracted as previously described [69] using TRIzol reagent according to the manufacturer's instructions (Thermo Fisher Scientific Inc.). The purity and integrity of the obtained RNAs was measured by Nanodrop (Thermo Fisher Scientific Inc.) and Bioanalyzer (Agilent Technologies). For mRNA and lncRNA analysis, rRNA depletion and library preparation were performed following manufacturer instruction for the Nugen OVATION RNA-Seq System V2 and Nugen OVATION Ultralow Library Systems (rRNA-depleted RNA-sequencing). For miRNA analysis, extraction and library preparation were performed following manufacturer instruction for the TruSeq Small RNA Library Preparation Kit. An Illumina HiSeq 2500 was used to perform a paired-end sequencing with 100 bp long reads (small RNA-sequencing). The average estimated insert size for mRNA and lncRNA was 150 bp. Small RNA libraries were sequenced twice.

RNA-sequencing data analysis

FastQC (http://www.bioinformatics.babraham.ac.uk/ projects/fastqc, version 0.11.3) was used for quality

control for both long and short RNA datasets. For mRNA and lncRNA analysis, datasets were aligned on human hg19 reference genome using STAR [70] aligner (version 2.5.3a). Gene level differential expression analysis was done counting on hg19 annotation using FeatureCounts (https://www.r-project.org/) [71] in the Rsubread package and using the counts for a standard limma-voom [72] analysis. LncRNAs were identified using the biotypes indicated by ENSEMBL. Genes, both coding and noncoding, displaying ≥1 cpm in at least 3 samples were considered as expressed.

For miRNA analysis, reads were trimmed using Trimmomatic [73] software set for trimming adapters and regions with low quality scores. Only one mate for each pair and only reads longer than 15bp were retained. Datasets were aligned on human hg19 reference genome using BWA [74] aligner (version 0.7.12-r1039) and miRNAs differential expression was calculated using mirBase v20 database [75] and a standard limma approach. Linear model was set to take into account both the batch effect within the three available HUVEC batches and between two sequencing rounds. miRNAs displaying ≥ 10 reads every 10M reads in at least 3 samples in both sequencing rounds were considered as expressed.

For all RNA species, events were defined as significant using a cutoff of adjusted p value <0.05.

Data availability

Sequencing libraries are available on Gene Expression Omnibus [76] database under the accession number GSE104666. The superseries links to both the long and short RNA datasets. Available data comprise raw FASTQ and processed counts.

Gene expression bioinformatic analysis

Enrichment in GO terms from the Biological Process tree and KEGG pathways was calculated using ClueGO [21] app for Cytoscape [28], set to report terms with a corrected p value <0.05.

For MDM2 isoform-level differential expression analysis, DEXSeq [77] was used; results were confirmed using SwitchSeq (https://github.com/ mgonzalezporta/SwitchSeq) and transcript-level analysis by VastTools (http://vastdb.crg.eu) [78]. Events were defined as significant using a cutoff of p value <0.05. Further details on the regions involved and their coverage were manually gathered with the help of IGV browser [79].

For miRNA-target interactions, full list of known, validated miRNA-target interactions was downloaded from miRTarBase [27] website. The full database was intersected with the lists of significant miRNAs and mRNAs, retaining only miRNA-target couples showing opposite modulation in HUVEC cells under oxidative stress. Visual representation of the network of interaction was created in Cytoscape. Enrichment analysis was performed with ClueGO as described above on both the full list of modulated targets and on the targets of each single miRNA, separately.

p53 ChIP-seq analysis

ChIP-Seq datasets for human U2OS osteosarcoma cells treated with nutilin were downloaded from GEO (GSE46641) [34].

Reads were aligned on human hg19 reference genome using Bowtie2 (version 2.2.8) and subsequently used for a standard narrow-peak detection analysis using MACS2 (version 2.1.1.20160309). Peaks were detected providing untreated as background and were reported only when having a FDR<0.001. Genomic sequence under the peak was extracted using custom R scripts. p53 consensus was downloaded from Jaspar [80] and matched to the genomic sequence under the peak using custom R scripts.

Patient recruitment and classification

All studies were conducted in accordance with the ethical principles that have their origins in the Declaration of Helsinki.

For experiments with LLI subjects, 56 LLIs (older than 90 years of age) were enrolled by home visiting from community-dwelling people based in a rural area of southern Italy (Cilento) and anamnestic information was collected (Table S1) [38, 39]. Among LLIs, 28 presented systemic diseases (diabetes mellitus, hypertension, cardiovascular diseases, Alzheimer or senile dementia, respiratory diseases, rheumatoid arthritis) and were sub-classified as frail. Controls were 65 healthy donors recruited in the same geographic area of the LLIs, with an age range between 20 and 80 years old. All subjects were recruited in the same period of time and the collected blood samples were processed within 24h since collection. All subjects gave written informed consent to the study, which was approved by IRCCS MultiMedica Ethical Committee, CE/CE/42/ 2010/LDC, protocol N. "19 2010 Cardiovascolare".

For experiments with CLI subjects, skeletal muscle biopsies were harvested from 7 patients, 3 males and 4 females, aged 74.4 ±4.6 years, affected by terminal CLI and/or gangrene of the leg and undergoing above the knee amputation. Samples were placed in RNAlater (Qiagen) and frozen or processed within 24 hrs. Ischemic tibialis anterior muscle samples were compared to sartorius samples harvested at the amputation site of the same patient. The study was approved by the IRCCS-San Raffaele ethical committee, protocol code miRNACLI, number 69/INT/2016.

PBMC isolation

Peripheral blood (15mL) was collected through a forearm vein puncture and PBMCs were separated on Histopaque-1077 (Sigma-Aldrich) gradient at 1200xg.

RNA extraction and qPCR

Total RNA from tissues and cultured cells was extracted using TRIzol (Thermo Fisher Scientific Inc.) as described previously (Greco 2017). For LLIs study, RNA was extracted using miRNeasy kit (Qiagen) following the manufacturer's instructions. Sizing, quantitation and quality of the extracted RNAs was checked by Nanodrop ND-1000 (Nanodrop, Thermo Fisher Scientific Inc.) and Bioanalyzer 2100 (Agilent Technologies).

For mRNA and lncRNA qPCR experiments, RNA was retro-transcribed using the SuperScript III Reverse Transcriptase kit (Thermo Fisher Scientific Inc.) according to the manufacturer's instructions. cDNAs were analyzed using the SYBR-GREEN qPCR method (Thermo Fisher Scientific Inc.) according to the manufacturer's instructions. Sequences of the primers are reported in Table S2. Data were normalized to 18s rRNA levels in LLI experiments and to average UBC and RPL23A levels for all other experiments. For miRNA qPCR experiments, miRNAs were measured using Taqman MicroRNA single assays (Applied Biosystems) as previously described [81]. Samples were normalized in H_2O_2-treatment experiments to miR-25 expression, identified as suitable by small RNA-sequencing data analysis. For all other experiments, miR-16 was used as normalizer.

For all RNA species, relative expression was calculated using the $2^{-\Delta\Delta Ct}$ method [82].

Statistical analysis

GraphPad Prism v.4.03 software (GraphPad Software Inc.) and STATA 12 software (StataCorp. 2011. Stata Statistical Software: Release 12) were used for statistical analysis. Continuous variables were analyzed by Student's t-test, Mann-Whitney test or ANOVA, as opportune. Categorical variables were compared using

the Fisher's exact test and the chi-squared test. For experiments with LLI patients, a linear regression model was used to detect the genes and miRNAs expression levels that resulted significantly associated with life-span and heath-span after adjustment by sex. Expression levels were analyzed as $\log_2$ values since their distribution was positively skewed.

All statistical tests were performed 2-sided and a p <0.05 was considered as statistically significant. Continuous variables were expressed as mean ± standard error of the mean (SEM).

Abbreviations

BrdU: bromodeoxyuridine; ChIP-seq: ChIP-sequencing; CLI: critical limb ischemia; EC: endothelial cell; FDR: False Discovery Rate; LLIs: long-living individuals; lncRNAs: long noncoding-RNAs; miRNAs:microRNAs; ncRNAs: noncoding-RNAs; PBMCs: peripheral blood mononuclear cells; SEM: standard error of the mean.

AUTHOR CONTRIBUTIONS

PF and FM designed the study and wrote the manuscript. CG, AAP, GS and AM advised on the study. PF CV, ES, MP performed experiments. MC, and JMGM performed bioinformatics and CS statistics. PR, BM, FV, GN collected clinical samples and parameters. All authors contributed to editing and proofreading, approving the final manuscript.

ACKNOWLEDGEMENTS

CONFLICTS OF INTEREST

The authors declare no conflicts of interest.

FUNDING

REFERENCES

1. Incalza MA, D'Oria R, Natalicchio A, Perrini S, Laviola L, Giorgino F. Oxidative stress and reactive oxygen species in endothelial dysfunction associated with cardiovascular and metabolic diseases. Vascul Pharmacol. 2017. Epub ahead of print. https://doi.org/10.1016/j.vph.2017.05.005

2. Magenta A, Greco S, Capogrossi MC, Gaetano C, Martelli F. Nitric oxide, oxidative stress, and p66Shc interplay in diabetic endothelial dysfunction. BioMed Res Int. 2014; 2014:193095. https://doi.org/10.1155/2014/193095

3. Handy DE, Loscalzo J. Responses to reductive stress in the cardiovascular system. Free Radic Biol Med. 2017; 109:114–24. https://doi.org/10.1016/j.freeradbiomed.2016.12.006

4. Klotz LO, Sánchez-Ramos C, Prieto-Arroyo I, Urbánek P, Steinbrenner H, Monsalve M. Redox regulation of FoxO transcription factors. Redox Biol. 2015; 6:51–72. https://doi.org/10.1016/j.redox.2015.06.019

5. Kastenhuber ER, Lowe SW. Putting p53 in Context. Cell. 2017; 170:1062–78. https://doi.org/10.1016/j.cell.2017.08.028

6. Eman MR, Regan-Klapisz E, Pinkse MW, Koop IM, Haverkamp J, Heck AJ, Verkleij AJ, Post JA. Protein expression dynamics during replicative senescence of endothelial cells studied by 2-D difference in-gel electrophoresis. Electrophoresis. 2006; 27:1669–82. https://doi.org/10.1002/elps.200500746

7. Unterluggauer H, Hampel B, Zwerschke W, Jansen-Dürr P. Senescence-associated cell death of human endothelial cells: the role of oxidative stress. Exp Gerontol. 2003; 38:1149–60. https://doi.org/10.1016/j.exger.2003.08.007

8. Erusalimsky JD, Skene C. Mechanisms of endothelial senescence. Exp Physiol. 2009; 94:299–304. https://doi.org/10.1113/expphysiol.2008.043133

9. Magenta A, Greco S, Gaetano C, Martelli F. Oxidative stress and microRNAs in vascular diseases. Int J Mol Sci. 2013; 14:17319–46. https://doi.org/10.3390/ijms140917319

10. Steven S, Daiber A, Dopheide JF, Münzel T, Espinola-Klein C. Peripheral artery disease, redox signaling, oxidative stress - Basic and clinical aspects. Redox Biol. 2017; 12:787–97. https://doi.org/10.1016/j.redox.2017.04.017

11. Greco S, Gorospe M, Martelli F. Noncoding RNA in age-related cardiovascular diseases. J Mol Cell Cardiol. 2015; 83:142–55. https://doi.org/10.1016/j.yjmcc.2015.01.011

12. Finkel T, Holbrook NJ. Oxidants, oxidative stress and the biology of ageing. Nature. 2000; 408:239–47. https://doi.org/10.1038/35041687

13. Harman D. Prolongation of the normal life span by radiation protection chemicals. J Gerontol. 1957;

12:257–63. https://doi.org/10.1093/geronj/12.3.257

14. Brandes RP, Weissmann N, Schröder K. Redox-mediated signal transduction by cardiovascular Nox NADPH oxidases. J Mol Cell Cardiol. 2014; 73:70–79. https://doi.org/10.1016/j.yjmcc.2014.02.006

15. Fuschi P, Maimone B, Gaetano C, Martelli F. Noncoding RNAs in the vascular system response to oxidative stress. Antioxid Redox Signal. 2017; Epub ahead of print. https://doi.org/10.1089/ars.2017.7229

16. Cech TR, Steitz JA. The noncoding RNA revolution-trashing old rules to forge new ones. Cell. 2014; 157:77–94. https://doi.org/10.1016/j.cell.2014.03.008

17. Fabian MR, Sonenberg N, Filipowicz W. Regulation of mRNA translation and stability by microRNAs. Annu Rev Biochem. 2010; 79:351–79. https://doi.org/10.1146/annurev-biochem-060308-103103

18. Carlomosti F, D'Agostino M, Beji S, Torcinaro A, Rizzi R, Zaccagnini G, Maimone B, Di Stefano V, De Santa F, Cordisco S, Antonini A, Ciarapica R, Dellambra E, et al. Oxidative stress-induced miR-200c disrupts the regulatory loop among SIRT1, FOXO1, and eNOS. Antioxid Redox Signal. 2017; 27:328–44. https://doi.org/10.1089/ars.2016.6643

19. Magenta A, Cencioni C, Fasanaro P, Zaccagnini G, Greco S, Sarra-Ferraris G, Antonini A, Martelli F, Capogrossi MC. miR-200c is upregulated by oxidative stress and induces endothelial cell apoptosis and senescence via ZEB1 inhibition. Cell Death Differ. 2011; 18:1628–39. https://doi.org/10.1038/cdd.2011.42

20. Goff LA, Rinn JL. Linking RNA biology to lncRNAs. Genome Res. 2015; 25:1456–65. https://doi.org/10.1101/gr.191122.115

21. Bindea G, Mlecnik B, Hackl H, Charoentong P, Tosolini M, Kirilovsky A, Fridman WH, Pagès F, Trajanoski Z, Galon J, Clue GO. ClueGO: a Cytoscape plug-in to decipher functionally grouped gene ontology and pathway annotation networks. Bioinformatics. 2009; 25:1091–93. https://doi.org/10.1093/bioinformatics/btp101

22. Manfredi JJ. The Mdm2-p53 relationship evolves: Mdm2 swings both ways as an oncogene and a tumor suppressor. Genes Dev. 2010; 24:1580–89. https://doi.org/10.1101/gad.1941710

23. Inoue K, Fry EA. Aberrant splicing of the DMP1-ARF-MDM2-p53 pathway in cancer. Int J Cancer. 2016; 139:33–41. https://doi.org/10.1002/ijc.30003

24. Brown CY, Mize GJ, Pineda M, George DL, Morris DR. Role of two upstream open reading frames in the

25. translational control of oncogene mdm2. Oncogene. 1999; 18:5631–37. https://doi.org/10.1038/sj.onc.1202949

25. Cui M, You L, Ren X, Zhao W, Liao Q, Zhao Y. Long non-coding RNA PVT1 and cancer. Biochem Biophys Res Commun. 2016; 471:10–14. https://doi.org/10.1016/j.bbrc.2015.12.101

26. Barsotti AM, Beckerman R, Laptenko O, Huppi K, Caplen NJ, Prives C. p53-Dependent induction of PVT1 and miR-1204. J Biol Chem. 2012; 287:2509–19. https://doi.org/10.1074/jbc.M111.322875

27. Chou CH, Chang NW, Shrestha S, Hsu SD, Lin YL, Lee WH, Yang CD, Hong HC, Wei TY, Tu SJ, Tsai TR, Ho SY, Jian TY, et al. miRTarBase 2016: updates to the experimentally validated miRNA-target interactions database. Nucleic Acids Res. 2016; 44:D239–47. https://doi.org/10.1093/nar/gkv1258

28. Shannon P, Markiel A, Ozier O, Baliga NS, Wang JT, Ramage D, Amin N, Schwikowski B, Ideker T. Cytoscape: a software environment for integrated models of biomolecular interaction networks. Genome Res. 2003; 13:2498–504. https://doi.org/10.1101/gr.1239303

29. Noda T, Iwakiri R, Fujimoto K, Aw TY. Induction of mild intracellular redox imbalance inhibits proliferation of CaCo-2 cells. FASEB J. 2001; 15:2131–39. https://doi.org/10.1096/fj.01-0131com

30. Moore R, Ooi HK, Kang T, Bleris L, Ma L. MiR-192-mediated positive feedback loop controls the robustness of stress-induced p53 oscillations in breast cancer cells. PLOS Comput Biol. 2015; 11:e1004653. https://doi.org/10.1371/journal.pcbi.1004653

31. Braun CJ, Zhang X, Savelyeva I, Wolff S, Moll UM, Schepeler T, Ørntoft TF, Andersen CL, Dobbelstein M. p53-Responsive micrornas 192 and 215 are capable of inducing cell cycle arrest. Cancer Res. 2008; 68:10094–104. https://doi.org/10.1158/0008-5472.CAN-08-1569

32. Georges SA, Biery MC, Kim SY, Schelter JM, Guo J, Chang AN, Jackson AL, Carleton MO, Linsley PS, Cleary MA, Chau BN. Coordinated regulation of cell cycle transcripts by p53-Inducible microRNAs, miR-192 and miR-215. Cancer Res. 2008; 68:10105–12. https://doi.org/10.1158/0008-5472.CAN-08-1846

33. Song B, Wang Y, Kudo K, Gavin EJ, Xi Y, Ju J. miR-192 Regulates dihydrofolate reductase and cellular proliferation through the p53-microRNA circuit. Clin Cancer Res. 2008; 14:8080–86. https://doi.org/10.1158/1078-0432.CCR-08-1422

34. Menendez D, Nguyen TA, Freudenberg JM, Mathew VJ, Anderson CW, Jothi R, Resnick MA. Diverse

stresses dramatically alter genome-wide p53 binding and transactivation landscape in human cancer cells. Nucleic Acids Res. 2013; 41:7286–301. https://doi.org/10.1093/nar/gkt504

35. Abdelmohsen K, Gorospe M. Noncoding RNA control of cellular senescence. Wiley Interdisc Rev RNA. 2015; 6:615–29. https://doi.org/10.1002/wrna.1297

36. Nagy C, Maheu M, Lopez JP, Vaillancourt K, Cruceanu C, Gross JA, Arnovitz M, Mechawar N, Turecki G. Effects of postmortem interval on biomolecule integrity in the brain. J Neuropathol Exp Neurol. 2015; 74:459–69. https://doi.org/10.1097/NEN.0000000000000190

37. Dato S, Crocco P, D'Aquila P, de Rango F, Bellizzi D, Rose G, Passarino G. Exploring the role of genetic variability and lifestyle in oxidative stress response for healthy aging and longevity. Int J Mol Sci. 2013; 14:16443–72. https://doi.org/10.3390/ijms140816443

38. Villa F, Carrizzo A, Spinelli CC, Ferrario A, Malovini A, Maciąg A, Damato A, Auricchio A, Spinetti G, Sangalli E, Dang Z, Madonna M, Ambrosio M, et al. Genetic analysis reveals a longevity-associated protein modulating endothelial function and angiogenesis. Circ Res. 2015; 117:333–45. https://doi.org/10.1161/CIRCRESAHA.117.305875

39. Spinetti G, Sangalli E, Specchia C, Villa F, Spinelli C, Pipolo R, Carrizzo A, Greco S, Voellenkle C, Vecchione C, Madeddu P, Martelli F, Puca AA. The expression of the BPIFB4 and CXCR4 associates with sustained health in long-living individuals from Cilento-Italy. Aging (Albany NY). 2017; 9:370–80. https://doi.org/10.18632/aging.101159

40. Soysal P, Isik AT, Carvalho AF, Fernandes BS, Solmi M, Schofield P, Veronese N, Stubbs B. Oxidative stress and frailty: A systematic review and synthesis of the best evidence. Maturitas. 2017; 99:66–72. https://doi.org/10.1016/j.maturitas.2017.01.006

41. Fischer S, Wiesnet M, Renz D, Schaper W. H2O2 induces paracellular permeability of porcine brain-derived microvascular endothelial cells by activation of the p44/42 MAP kinase pathway. Eur J Cell Biol. 2005; 84:687–97. https://doi.org/10.1016/j.ejcb.2005.03.002

42. Haendeler J, Popp R, Goy C, Tischler V, Zeiher AM, Dimmeler S. Cathepsin D and H2O2 stimulate degradation of thioredoxin-1: implication for endothelial cell apoptosis. J Biol Chem. 2005; 280:42945–51. https://doi.org/10.1074/jbc.M506985200

43. Zadeh MS, Kolb JP, Geromin D, D'Anna R, Boulmerka A, Marconi A, Dugas B, Marsac C, D'Alessio P. Regulation of ICAM-1/CD54 expression on human endothelial cells by hydrogen peroxide involves inducible NO synthase. J Leukoc Biol. 2000; 67:327–34.

44. Valen G, Erl W, Eriksson P, Wuttge D, Paulsson G, Hansson GK. Hydrogen peroxide induces mRNA for tumour necrosis factor alpha in human endothelial cells. Free Radic Res. 1999; 31:503–12. https://doi.org/10.1080/10715769900301071

45. Sánchez-Gómez FJ, Calvo E, Bretón-Romero R, Fierro-Fernández M, Anilkumar N, Shah AM, Schröder K, Brandes RP, Vázquez J, Lamas S. NOX4-dependent Hydrogen peroxide promotes shear stress-induced SHP2 sulfenylation and eNOS activation. Free Radic Biol Med. 2015; 89:419–30. https://doi.org/10.1016/j.freeradbiomed.2015.08.014

46. Cicchillitti L, Fasanaro P, Biglioli P, Capogrossi MC, Martelli F. Oxidative stress induces protein phosphatase 2A-dependent dephosphorylation of the pocket proteins pRb, p107, and p130. J Biol Chem. 2003; 278:19509–17. https://doi.org/10.1074/jbc.M300511200

47. Fasanaro P, Magenta A, Zaccagnini G, Cicchillitti L, Fucile S, Eusebi F, Biglioli P, Capogrossi MC, Martelli F. Cyclin D1 degradation enhances endothelial cell survival upon oxidative stress. FASEB J. 2006; 20:1242–44. https://doi.org/10.1096/fj.05-4695fje

48. Magenta A, Fasanaro P, Romani S, Di Stefano V, Capogrossi MC, Martelli F. Protein phosphatase 2A subunit PR70 interacts with pRb and mediates its dephosphorylation. Mol Cell Biol. 2008; 28:873–82. https://doi.org/10.1128/MCB.00480-07

49. Mathru M, Dries DJ, Barnes L, Tonino P, Sukhani R, Rooney MW. Tourniquet-induced exsanguination in patients requiring lower limb surgery. An ischemia-reperfusion model of oxidant and antioxidant metabolism. Anesthesiology. 1996; 84:14–22. https://doi.org/10.1097/00000542-199601000-00003

50. Slezak J, Tribulova N, Pristacova J, Uhrik B, Thomas T, Khaper N, Kaul N, Singal PK. Hydrogen peroxide changes in ischemic and reperfused heart. Cytochemistry and biochemical and X-ray microanalysis. Am J Pathol. 1995; 147:772–81.

51. Granger DN, Kvietys PR. Reperfusion injury and reactive oxygen species: the evolution of a concept. Redox Biol. 2015; 6:524–51. https://doi.org/10.1016/j.redox.2015.08.020

52. Park WH. The effects of exogenous H2O2 on cell death, reactive oxygen species and glutathione levels in calf pulmonary artery and human umbilical vein endothelial cells. Int J Mol Med. 2013; 31:471–76. https://doi.org/10.3892/ijmm.2012.1215

53. Yue X, Acun A, Zorlutuna P. Transcriptome profiling of 3D co-cultured cardiomyocytes and endothelial cells under oxidative stress using a photocrosslinkable hydrogel system. Acta Biomater. 2017; 58:337–48. https://doi.org/10.1016/j.actbio.2017.06.031

54. Zhou Y, Zhong Y, Wang Y, Zhang X, Batista DL, Gejman R, Ansell PJ, Zhao J, Weng C, Klibanski A. Activation of p53 by MEG3 non-coding RNA. J Biol Chem. 2007; 282:24731–42. https://doi.org/10.1074/jbc.M702029200

55. Zhan R, Xu K, Pan J, Xu Q, Xu S, Shen J. Long noncoding RNA MEG3 mediated angiogenesis after cerebral infarction through regulating p53/NOX4 axis. Biochem Biophys Res Commun. 2017; 490:700–06. https://doi.org/10.1016/j.bbrc.2017.06.104

56. Adriaens C, Standaert L, Barra J, Latil M, Verfaillie A, Kalev P, Boeckx B, Wijnhoven PW, Radaelli E, Vermi W, Leucci E, Lapouge G, Beck B, et al. p53 induces formation of NEAT1 lncRNA-containing paraspeckles that modulate replication stress response and chemosensitivity. Nat Med. 2016; 22:861–68. https://doi.org/10.1038/nm.4135

57. Tripathi V, Shen Z, Chakraborty A, Giri S, Freier SM, Wu X, Zhang Y, Gorospe M, Prasanth SG, Lal A, Prasanth KV. Long noncoding RNA MALAT1 controls cell cycle progression by regulating the expression of oncogenic transcription factor B-MYB. PLoS Genet. 2013; 9:e1003368. https://doi.org/10.1371/journal.pgen.1003368

58. Mello SS, Sinow C, Raj N, Mazur PK, Bieging-Rolett K, Broz DK, Imam JF, Vogel H, Wood LD, Sage J, Hirose T, Nakagawa S, Rinn J, Attardi LD. Neat1 is a p53-inducible lincRNA essential for transformation suppression. Genes Dev. 2017; 31:1095–108. https://doi.org/10.1101/gad.284661.116

59. Takei Y, Ishikawa S, Tokino T, Muto T, Nakamura Y. Isolation of a novel TP53 target gene from a colon cancer cell line carrying a highly regulated wild-type TP53 expression system. Genes Chromosomes Cancer. 1998; 23:1–9. https://doi.org/10.1002/(SICI)1098-2264(199809)23:1<1::AID-GCC1>3.0.CO;2-Y

60. Ma XY, Wang JH, Wang JL, Ma CX, Wang XC, Liu FS. Malat1 as an evolutionarily conserved lncRNA, plays a positive role in regulating proliferation and maintaining undifferentiated status of early-stage hematopoietic cells. BMC Genomics. 2015; 16:676. https://doi.org/10.1186/s12864-015-1881-x

61. Pichiorri F, Suh SS, Rocci A, De Luca L, Taccioli C, Santhanam R, Zhou W, Benson DM Jr, Hofmainster C, Alder H, Garofalo M, Di Leva G, Volinia S, et al. Downregulation of p53-inducible microRNAs 192, 194, and 215 impairs the p53/MDM2 autoregulatory loop in multiple myeloma development. Cancer Cell. 2010; 18:367–81. https://doi.org/10.1016/j.ccr.2010.09.005

62. Donato AJ, Morgan RG, Walker AE, Lesniewski LA. Cellular and molecular biology of aging endothelial cells. J Mol Cell Cardiol. 2015; 89:122–35. https://doi.org/10.1016/j.yjmcc.2015.01.021

63. Zaccagnini G, Martelli F, Fasanaro P, Magenta A, Gaetano C, Di Carlo A, Biglioli P, Giorgio M, Martin-Padura I, Pelicci PG, Capogrossi MC. p66ShcA modulates tissue response to hindlimb ischemia. Circulation. 2004; 109:2917–23. https://doi.org/10.1161/01.CIR.0000129309.58874.0F

64. Yu B, Shan G. Functions of long noncoding RNAs in the nucleus. Nucleus. 2016; 7:155–66. https://doi.org/10.1080/19491034.2016.1179408

65. Choudhry H, Albukhari A, Morotti M, Haider S, Moralli D, Smythies J, Schödel J, Green CM, Camps C, Buffa F, Ratcliffe P, Ragoussis J, Harris AL, Mole DR. Tumor hypoxia induces nuclear paraspeckle formation through HIF-2α dependent transcriptional activation of NEAT1 leading to cancer cell survival. Oncogene. 2015; 34:4482–90. https://doi.org/10.1038/onc.2014.378

66. Voellenkle C, Rooij J, Guffanti A, Brini E, Fasanaro P, Isaia E, Croft L, David M, Capogrossi MC, Moles A, Felsani A, Martelli F. Deep-sequencing of endothelial cells exposed to hypoxia reveals the complexity of known and novel microRNAs. RNA. 2012; 18:472–84. https://doi.org/10.1261/rna.027615.111

67. West JA, Davis CP, Sunwoo H, Simon MD, Sadreyev RI, Wang PI, Tolstorukov MY, Kingston RE. The long noncoding RNAs NEAT1 and MALAT1 bind active chromatin sites. Mol Cell. 2014; 55:791–802. https://doi.org/10.1016/j.molcel.2014.07.012

68. Menghini R, Casagrande V, Marino A, Marchetti V, Cardellini M, Stoehr R, Rizza S, Martelli E, Greco S, Mauriello A, Ippoliti A, Martelli F, Lauro R, Federici M. MiR-216a: a link between endothelial dysfunction and autophagy. Cell Death Dis. 2014; 5:e1029. https://doi.org/10.1038/cddis.2013.556

69. Voellenkle C, Garcia-Manteiga JM, Pedrotti S, Perfetti A, De Toma I, Da Silva D, Maimone B, Greco S, Fasanaro P, Creo P, Zaccagnini G, Gaetano C, Martelli F. Implication of Long noncoding RNAs in the endothelial cell response to hypoxia revealed by RNA-sequencing. Sci Rep. 2016; 6:24141. https://doi.org/10.1038/srep24141

70. Dobin A, Davis CA, Schlesinger F, Drenkow J, Zaleski C, Jha S, Batut P, Chaisson M, Gingeras TR. STAR:

ultrafast universal RNA-seq aligner. Bioinformatics. 2013; 29:15–21.
https://doi.org/10.1093/bioinformatics/bts635

71. Liao Y, Smyth GK, Shi W. featureCounts: an efficient general purpose program for assigning sequence reads to genomic features. Bioinformatics. 2014; 30:923–30.
https://doi.org/10.1093/bioinformatics/btt656

72. Ritchie ME, Phipson B, Wu D, Hu Y, Law CW, Shi W, Smyth GK. limma powers differential expression analyses for RNA-sequencing and microarray studies. Nucleic Acids Res. 2015; 43:e47.
https://doi.org/10.1093/nar/gkv007

73. Bolger AM, Lohse M, Usadel B. Trimmomatic: a flexible trimmer for Illumina sequence data. Bioinformatics. 2014; 30:2114–20.
https://doi.org/10.1093/bioinformatics/btu170

74. Li H, Durbin R. Fast and accurate long-read alignment with Burrows-Wheeler transform. Bioinformatics. 2010; 26:589–95.
https://doi.org/10.1093/bioinformatics/btp698

75. Kozomara A, Griffiths-Jones S. miRBase: annotating high confidence microRNAs using deep sequencing data. Nucleic Acids Res. 2014; 42:D68–73.
https://doi.org/10.1093/nar/gkt1181

76. Barrett T, Wilhite SE, Ledoux P, Evangelista C, Kim IF, Tomashevsky M, Marshall KA, Phillippy KH, Sherman PM, Holko M, Yefanov A, Lee H, Zhang N, et al. NCBI GEO: archive for functional genomics data sets--update. Nucleic Acids Res. 2013; 41:D991–95.
https://doi.org/10.1093/nar/gks1193

77. Anders S, Reyes A, Huber W. Detecting differential usage of exons from RNA-seq data. Genome Res. 2012; 22:2008–17.
https://doi.org/10.1101/gr.133744.111

78. Irimia M, Weatheritt RJ, Ellis JD, Parikshak NN, Gonatopoulos-Pournatzis T, Babor M, Quesnel-Vallières M, Tapial J, Raj B, O'Hanlon D, Barrios-Rodiles M, Sternberg MJ, Cordes SP, et al. A highly conserved program of neuronal microexons is misregulated in autistic brains. Cell. 2014; 159:1511–23. https://doi.org/10.1016/j.cell.2014.11.035

79. Robinson JT, Thorvaldsdóttir H, Winckler W, Guttman M, Lander ES, Getz G, Mesirov JP. Integrative genomics viewer. Nat Biotechnol. 2011; 29:24–26.
https://doi.org/10.1038/nbt.1754

80. Mathelier A, Fornes O, Arenillas DJ, Chen CY, Denay G, Lee J, Shi W, Shyr C, Tan G, Worsley-Hunt R, Zhang AW, Parcy F, Lenhard B, et al. JASPAR 2016: a major expansion and update of the open-access database of transcription factor binding profiles. Nucleic Acids Res. 2016; 44:D110–15.
https://doi.org/10.1093/nar/gkv1176

81. Greco S, Perfetti A, Fasanaro P, Cardani R, Capogrossi MC, Meola G, Martelli F. Deregulated microRNAs in myotonic dystrophy type 2. PLoS One. 2012; 7:e39732.
https://doi.org/10.1371/journal.pone.0039732

82. Livak KJ, Schmittgen TD. Analysis of relative gene expression data using real-time quantitative PCR and the 2(-Delta Delta C(T)) Method. Methods. 2001; 25:402–08. https://doi.org/10.1006/meth.2001.1262

SUPPLEMENTARY MATERIAL

Table S1. LLI study population (N=118).

Group	n	Age mean (SD)	Age range	Sex (M/F)
Controls	65	49.2 (14.2)	25-78	24/41
LLIs	53	98.2 (4.1)	91-107	18/35
Frail-LLIs	28	97.9 (3.7)	91-104	14/14
Healthy-LLIs	25	98.5 (4.5)	91-107	4/21

Non-Healthy-LLIs, frail long-living individuals affected with diabetes, hypertension, cardiovascular disease, Alzheimer's disease, senile dementia, respiratory diseases or rheumatoid arthritis; Healthy-LLIs, healthy-aged long-living individuals; LLIs, all long-living individuals.*LLIs vs controls p=0.7 Healthy vs Non-healthy LLIs p=0.01.

Table S2. qPCR primers.

CDC25A	**F**	AATGGGCTCCTCCGAGTCAA
	R	TTCTTTACTGTCCAATGGCCC
CDKN1A	**F**	TGAGCCGCGACTGTGATG
	R	GTCTCGGTGACAAAGTCGAAGTT
FAS	**F**	ATGCCCAAGTGACTGACATCAA
	R	CTGGAGGACAGGGCTTATGG
GADD45A	**F**	AATTCTCGGCTGGAGAGCAG
	R	CTTCGTACACCCCGACAGTG
MDM2 exon1a	**F**	CGAAAACCCCGGATGGTGAG
	R	CGAAGCTGGAATCTGTGAGGT
MDM2 exon1b	**F**	AGTGGCGATTGGAGGGTAGA
	R	GTCTCTTGTTCCGAAGCTGGA
p53	**F**	CCCCAGCCAAAGAAGAAAC
	R	AACATCTCGAAGCGCTCAC
RAD51	**F**	TCATACGCTAGCTGTCACCTG
	R	AGCAGCCGTTCTGGCCTAA
C15orf5	**F**	CTGGAGTGAGGAGACTGAGGA
	R	CTTTTAAACCCACACCGCTTGA
DLEU2	**F**	AGCCAAATGTCCCATTTAAAGTT
	R	ATTGCTGAGCTAAGTAGAGGTC
GSN-AS1	**F**	GCCCCTGTGTCATAGTCACC
	R	CACAGTTAAGTGAGGGCCCAG
KIFC1	**F**	GAGGCCTGACCAGATGGAAG
	R	GGCACTGTAGTGAGGGATGG
LINC00702	**F**	AGAAAGGAGAAGAAAGTAGCTTGT
	R	GAAGTGCCTGTAGGAGATTCCA
MALAT1	**F**	TGTGTGCCAATGTTTCGTTT
	R	AGGAGAAAGTGCCATGGTTG
MEG3	**F**	CTGGGTCGGCTGAAGAACTG
NEAT1	**F**	GGCACCAGCATTTGTGGTT3
	R	ACAAGGCCTCAGAAATGGGG
PVT1 exon1a	**F**	CGGCACCTTCCAGTGGAT
	R	CCGTGTCTCCACAGGTCACA
PVT1 exon1b	**F**	TCCCGGAAGCTGCAGAAG
	R	CCAGGCCACGAGGTTTCTC
PVT1 exon3_1 (fig S5)	**F**	GGTGACCTTGGCACATACAG
	R	GTCCTGGCAGTAAAAGGGGAA
PVT1 exon3_2 (fig S6)	**F**	TGGCACATACAGCCATCATGA
	R	ACGTGCCAAGCAGCTCAAA

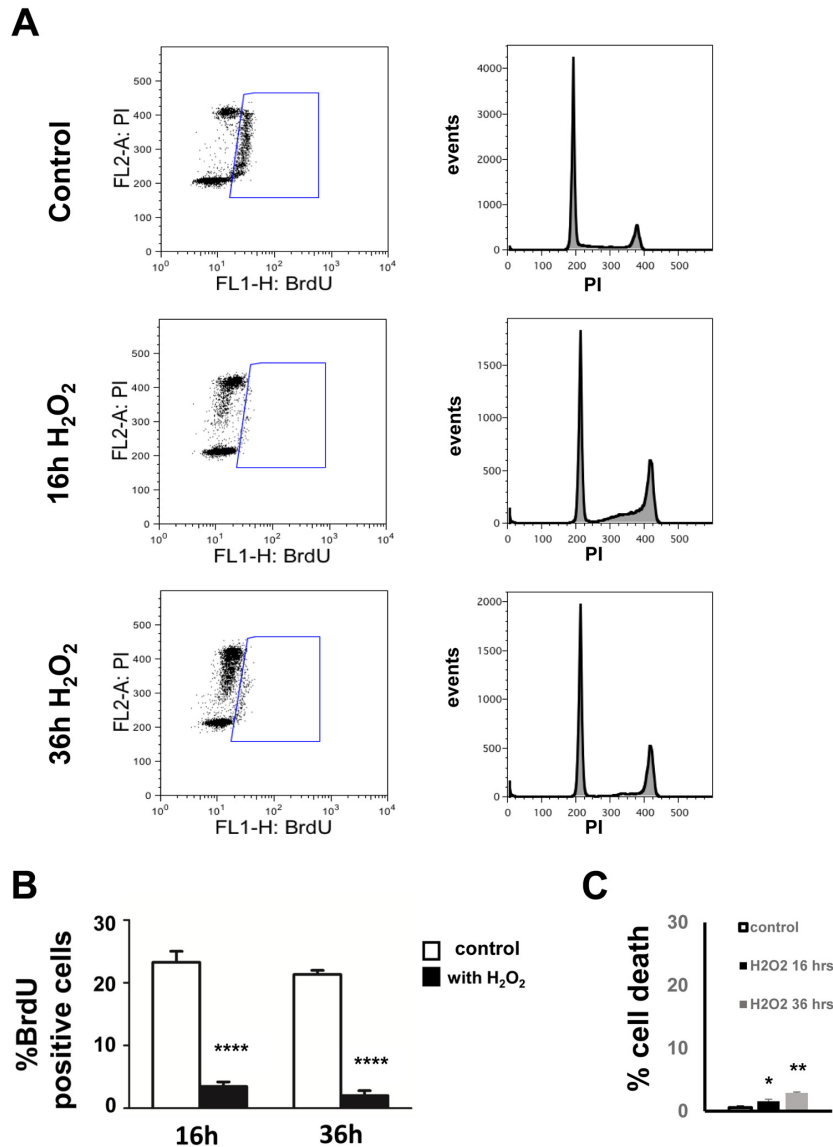| RAD51-AS1 | F | GCGAGTTTACAGACTGCCCT |
	R	GATGCATGCCGGGAGATGTA
TMPO	F	TGAAACTGAGGGAACAAGGAACA
	R	GCTCTGCCCTTTAGTGGTTCT
TP53TG1	F	ATTCCCAGTGAGCCGCTTTT
	R	GCTCTCAGAGTCCTTGGTGG

Figure S1. **Cell cycle analysis of H_2O_2–treated HUVEC used for RNA-sequencing profiling.** HUVEC were cultured with or without 200 μM H_2O_2 for 16 hrs and 36 hrs. Afterwards cells were pulse labelled with BrdU for 30 min before collecting, fixed and then stained with PI and α-BrdU antibody. (**A**) Representative images of BrdU incorporation (left panels) and PI staining (right panels), assessing DNA synthesis and DNA content, respectively, of HUVEC treated or not with H_2O_2 for 16 or 36 hrs. Pre-gated single cells were visualized in bivariate dot plots of BrdU vs PI to properly set the BrdU-positivity gates, thus taking into account the different autofluorescence of cells in the distinct phases of their cell cycle (left panels). Univariate histograms of DNA-bound PI are also showed (right panels). (**B**) Bar graph representing average values ±SEM of BrdU incorporation shows a decrease in DNA synthesis in H_2O_2-treated HUVEC (n= 3; ***P<0.001). C) Bar graph representing average percentage ±SEM of sub-G1 cells shows a significant but small increase of cell death upon H_2O_2 treatment (n= 3; *p<0.05, **p<0.01).

A

CDKN1A

- □ control
- ■ 16h H₂O₂
- ■ 36h H₂O₂

B

ZEB1

- □ control
- ■ 16h H₂O₂
- ■ 36h H₂O₂
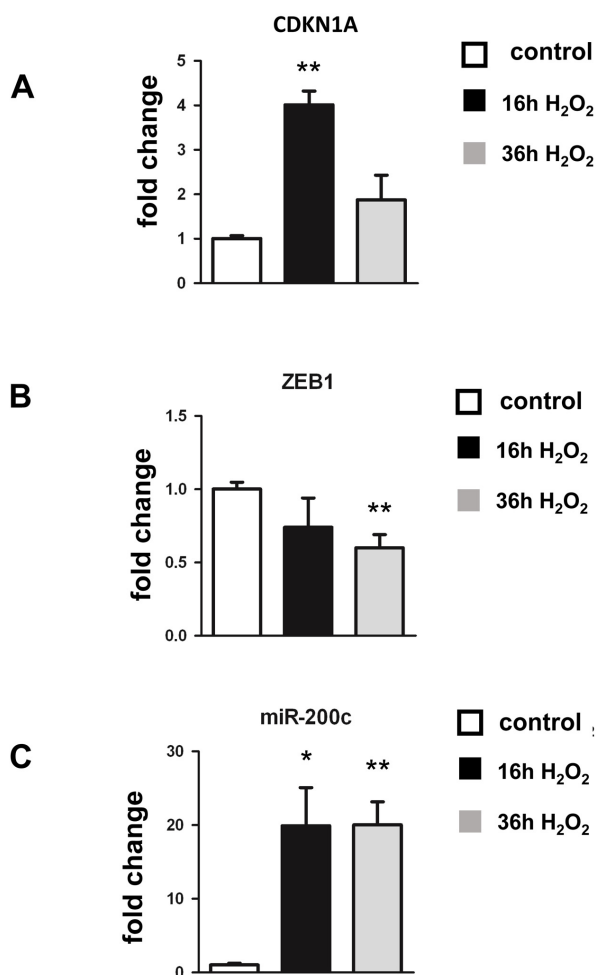
Figure S2. Positive controls in H₂O₂–treated HUVEC used for RNA-sequencing profiling. HUVEC were cultured with or without 200 μM H₂O₂ for 16 hrs and 36 hrs. Afterwards, total RNA was extracted and the indicated genes measured by qPCR. Average values are indicated ±SEM. A) The bar graph shows a significant increase of CDKN1A mRNA by 16 hrs of H₂O₂ treatment (n= 3; ***p<0.001). B) The bar graph shows a significant decrease of ZEB1 mRNA at 36 hrs of H₂O₂ treatment (n= 3; *p<0.05). C) The bar graph shows that miR-200c-3p was induced by H₂O₂ treatment (n= 3; *p<0.05; **p<0.01).

C

miR-200c

- □ control
- ■ 16h H₂O₂
- ■ 36h H₂O₂

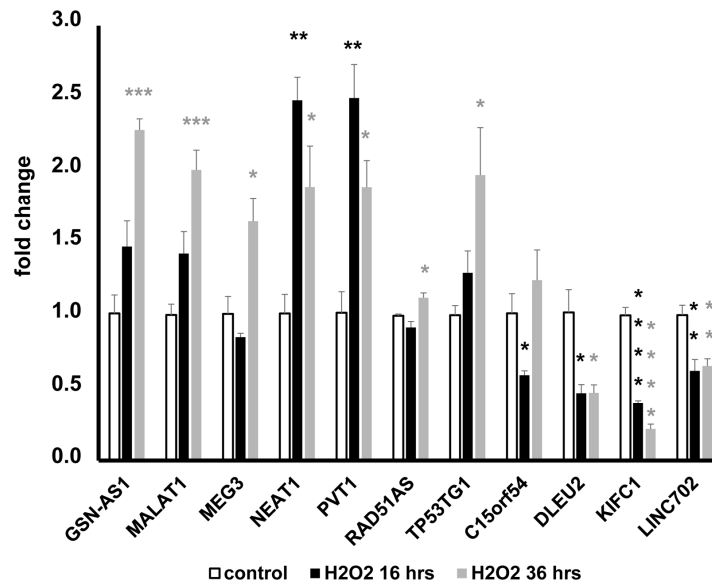- □ control
- ■ H2O2 16hrs
- ■ H2O2 36hrs
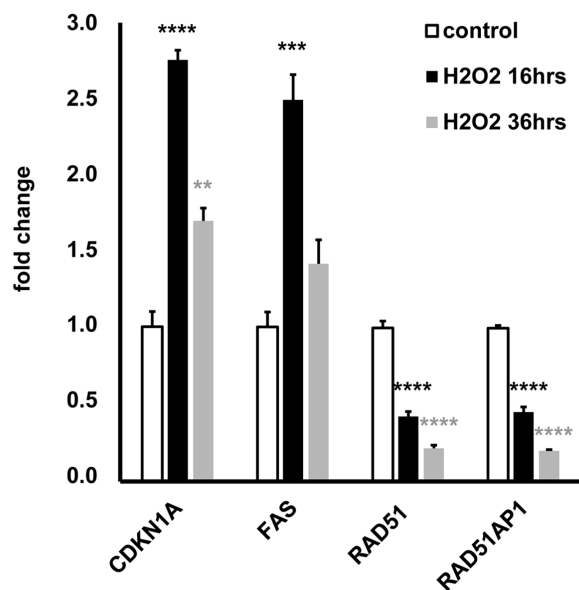
Figure S3. Validation of mRNAs differentially expressed upon HUVEC exposure to H₂O₂. HUVEC were exposed to H₂O₂ for 16 hrs and 36 hrs and the expression of the indicated mRNAs was measured by qPCR. The bar graph shows average ±SEM fold change values (n= 3; **p<0.01, ***p<0.001, ****p<0.0001).
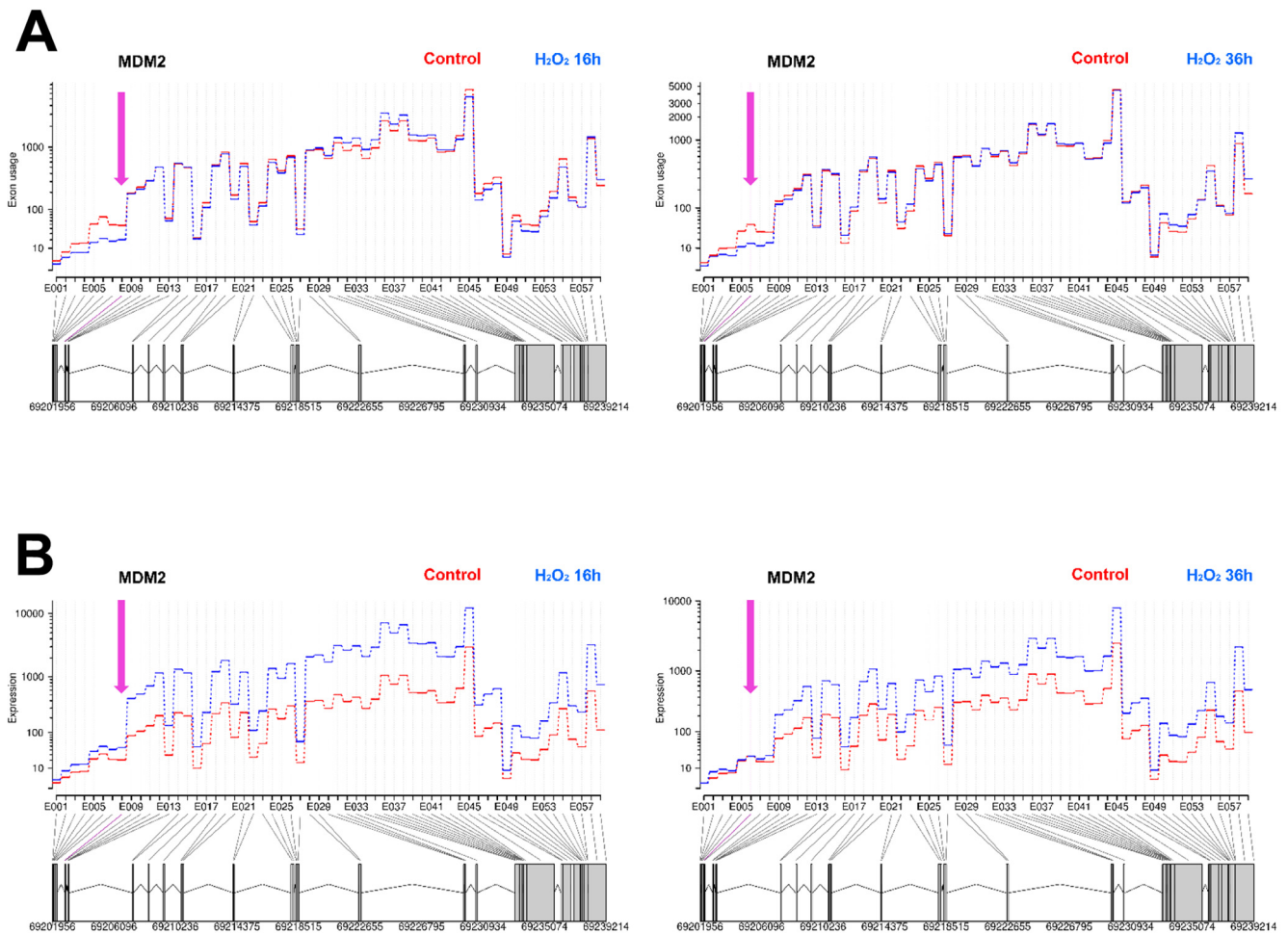
Figure S4. Alternative exon usage at the 5'UTR of MDM2. DEXSeq analysis of RNA-sequencing data reports a significant differential exon usage for the MDM2 gene at both 16 and 36 hrs of H_2O_2 HUVEC treatment. (**A**) Mean exon-level expression across replicates for both conditions was plotted against a schematic of all annotated exon fragments involved in a splicing event. The exon-level expression was in accord with the gene-level results that show a generalized increase of MDM2 gene in oxidative stress conditions. Expression upon H_2O_2 exposure was increased for all MDM2 exons but those at the 5' of the gene. (**B**) The same data are visualized normalizing expression values between all exon fragments of MDM2 to highlight differential exon usage at the 5' of the gene. Exon fragments displaying statistically significant differences are indicated by pink arrows (n= 3; p< 0.0001).

Figure S5. LncRNAs differentially expressed upon HUVEC exposure to H$_2$O$_2$. HUVEC were exposed to H$_2$O$_2$ for 16 hrs and 36 hrs and the expression of the indicated lncRNA was measured by qPCR. The bar graph shows average ±SEM fold change values expressed in a linear scale (n= 3; *p<0.05, **p<0.01, ***p<0.001, ****p<0.0001).
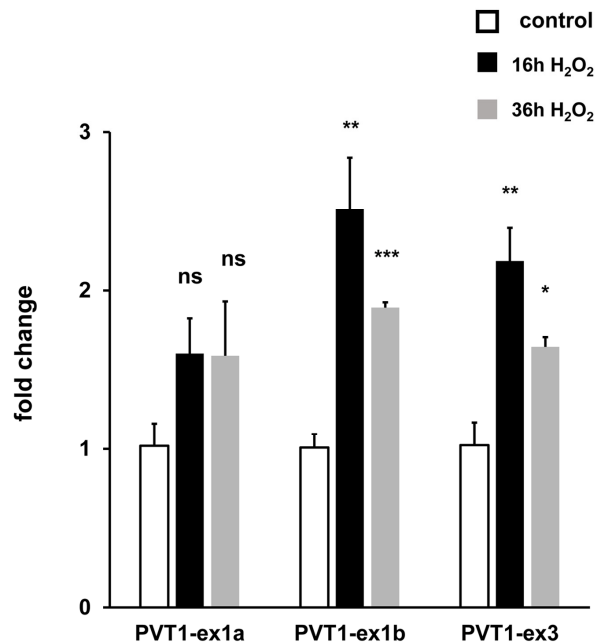

Figure S6. PVT1 alternative exon usage. HUVEC were exposed to H$_2$O$_2$ for 16 hrs and 36 hrs and the expression of the indicated PVT1 isoforms was measured by qPCR. In H$_2$O$_2$ treated HUVEC, exon 1b containing isoforms were induced. Modulation of exon 1a containing isoforms of PVT1 was not statistically significant. Primers detecting internal exon 3 were used as positive control. The bar graph shows average ±SEM fold change values (n= 3; *p<0.05, **p<0.01, **p<0.001).
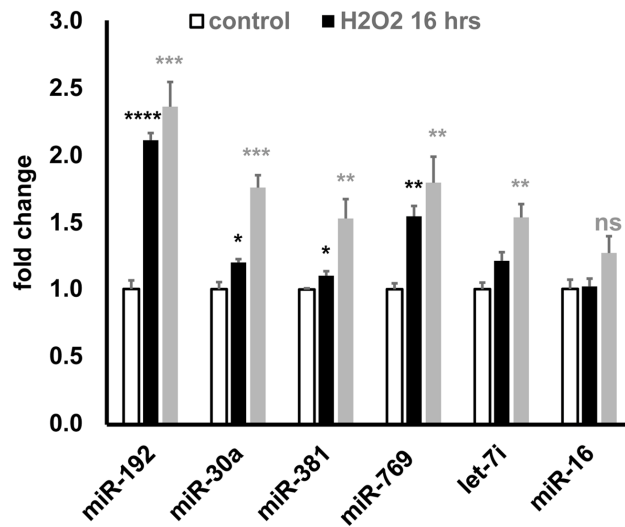
Figure S7. miRNAs differentially expressed upon HUVEC exposure to H₂O₂.
HUVEC were exposed to H₂O₂ for 16 hrs and 36 hrs and miRNA expression was measured by qPCR. The bar graph shows average ±SEM fold change values expressed in a linear scale (n= 3; *p<0.05, **p<0.01, ***p<0.001, ****p<0.0001, ns= not significant).
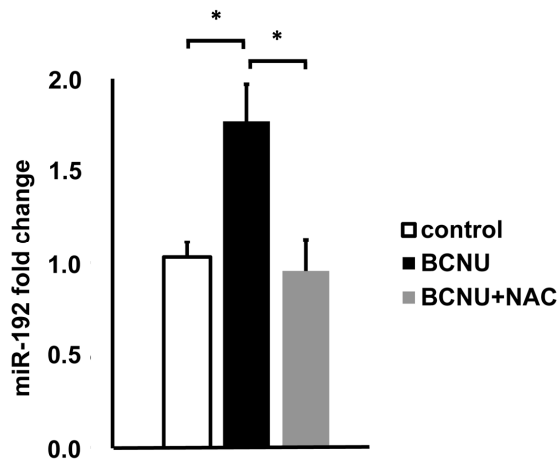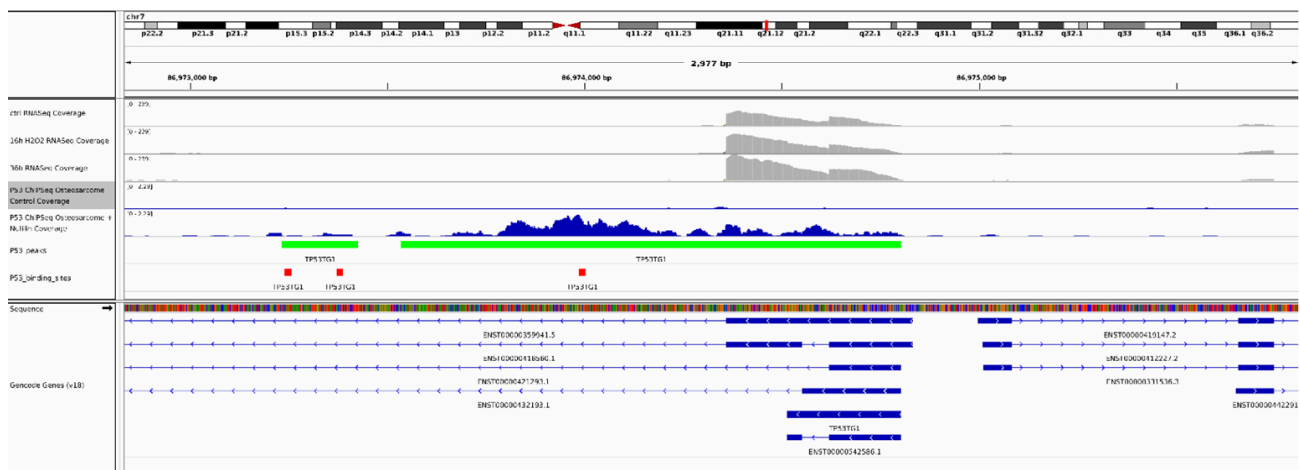

Figure S8. Redox imbalance induced by BCNU treatment induces miR-192-5p expression. HUVEC were either preincubated with 10 mM NAC or sham-treated for 30 min, followed by addition of 0.25 mM BCNU for 2 h. miR192-5p was measured by qPCR (n= 6; * p<0.05).
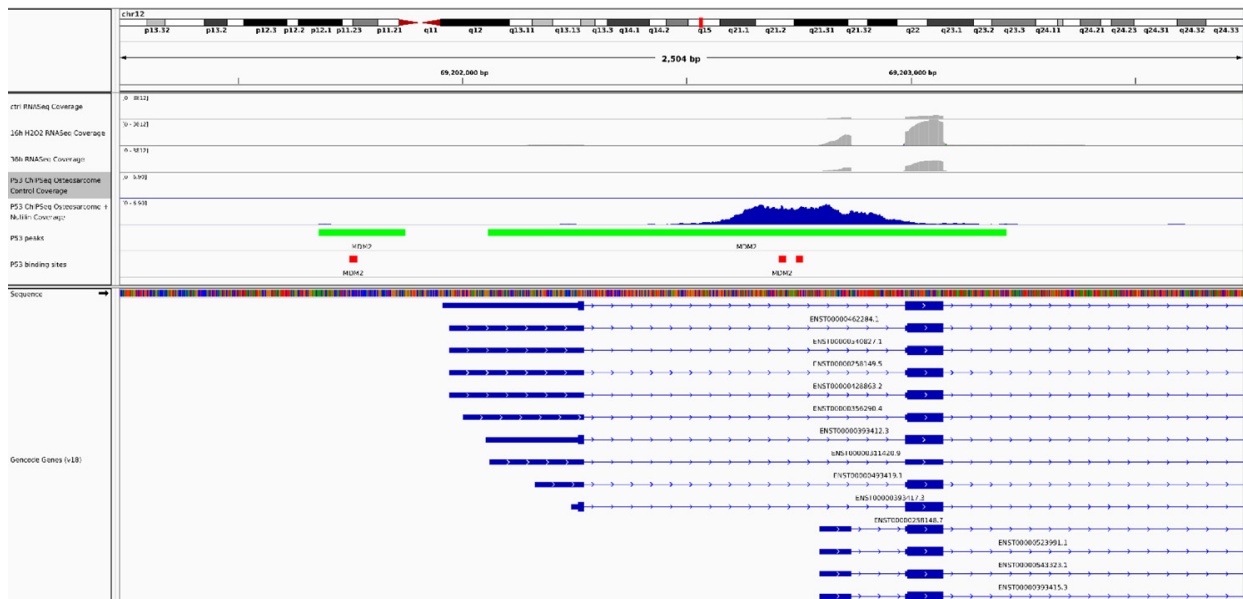
A CDKN1A
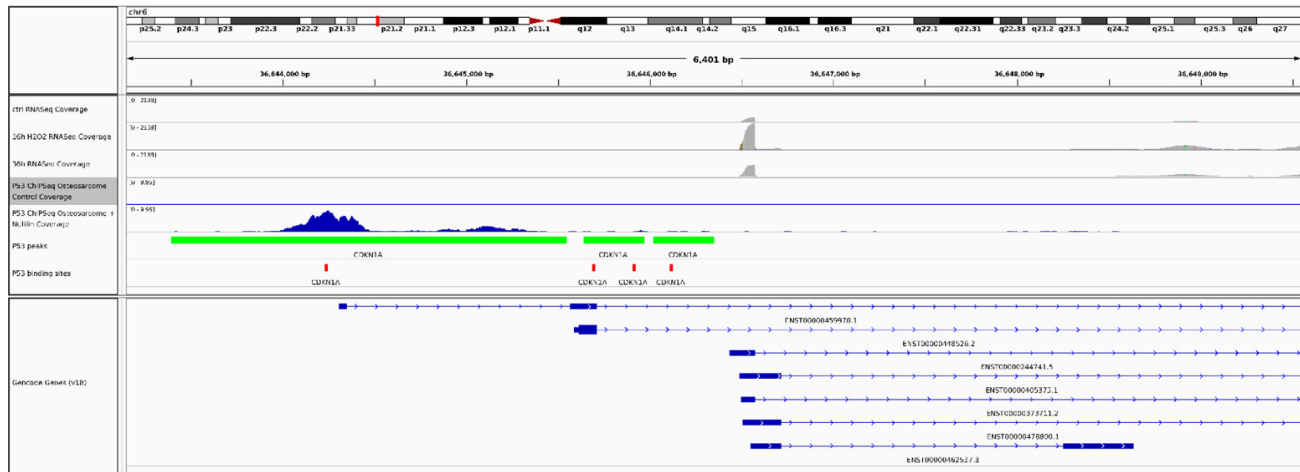
B GADD45A

C TP53TG1
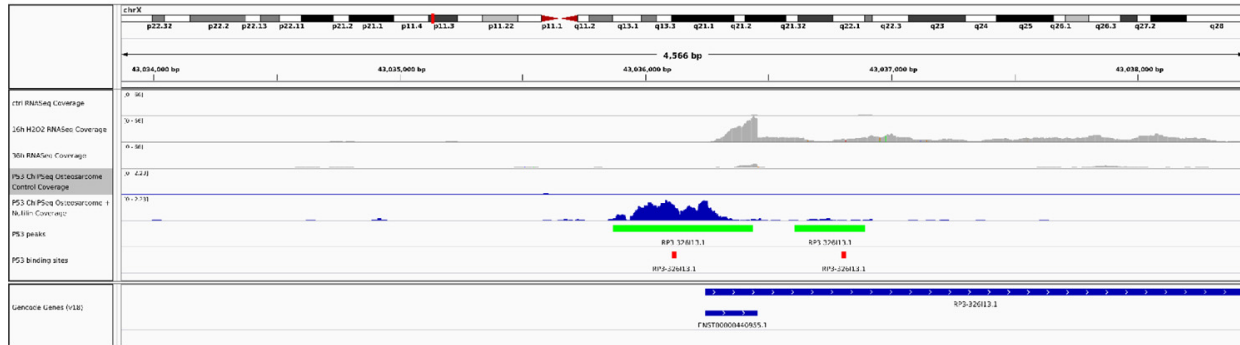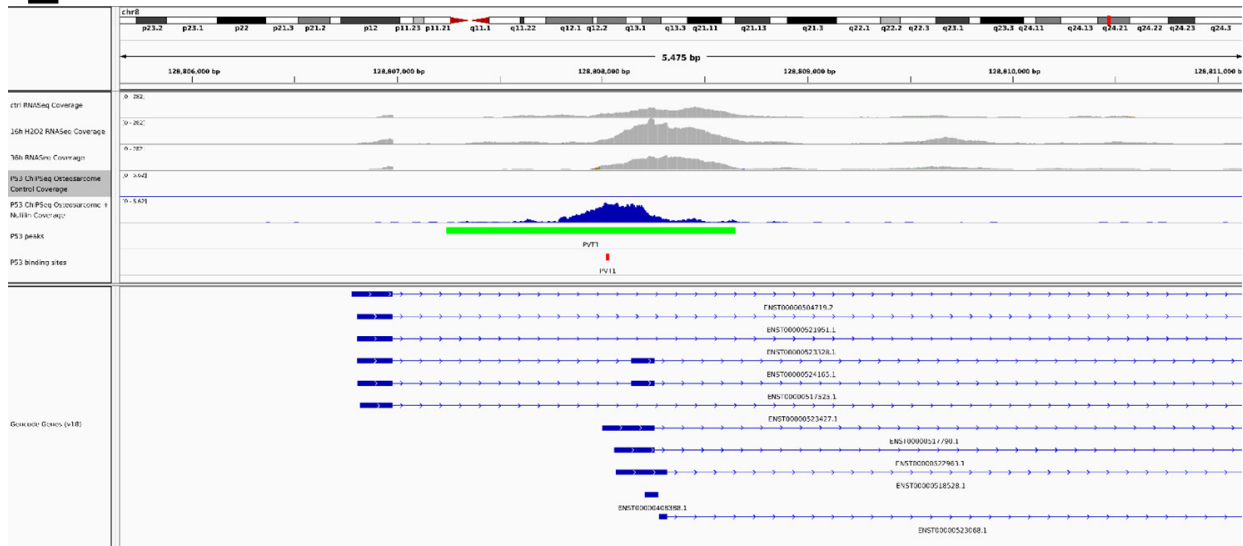
Figure S9. p53 occupancy in the regulatory regions of H₂O₂ modulated RNAs. Publicly available ChIP-seq data for p53 in osteosarcoma cells treated with nutilin, an activator of p53 (GSE46641) were analyzed. For each gene, the corresponding panel shows: genomic coordinates; reads in HUVEC treated with H₂O₂ for 0 hrs (ctrl), 16 hrs or 36 hrs (in gray); p53 ChIP-seq reads in control and nutilin treated osteosarcoma cells (in blue); significant (FDR<0.001) ChIP-seq peaks (green bars); consensus p53 binding sites (conservation ≥60%, in red); gencode annotated transcripts (in blue).
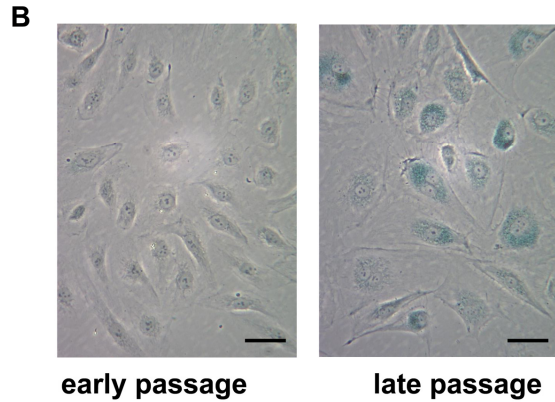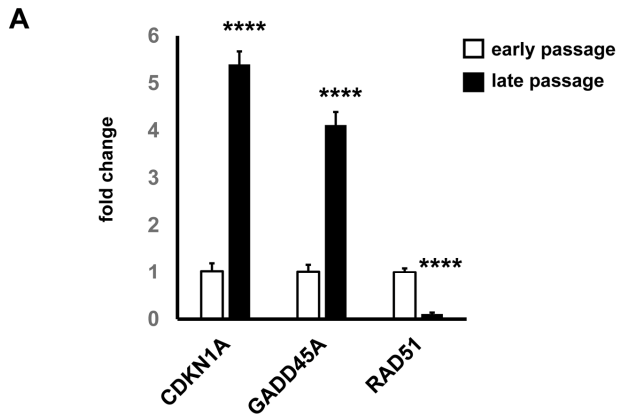
A

B

early passage   late passage

Figure S10. Senescence marker induction in late passage HUVEC. (**A**) Total RNA was extracted from early and late passage HUVEC and the indicated mRNAs were tested by qPCR. The bar graph shows average ±SEM fold change values (early passage n= 3, late passage n= 7; ****p<0.0001). (**B**) Representative pictures of early and late passage HUVEC stained for senescence-associated β-galactosidase activity (reference bar= 50μm).
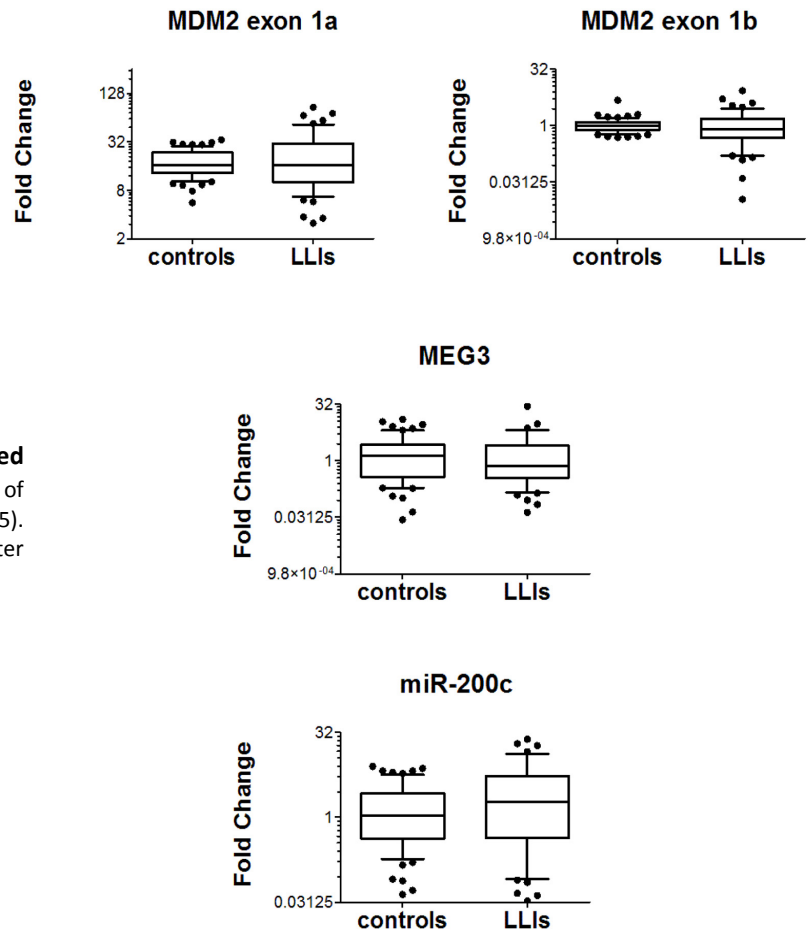
MDM2 exon 1a

MDM2 exon 1b

MEG3

miR-200c

Figure S11. Lack of association between the indicated H$_2$O$_2$-responsive RNA levels and life-span. Box plots of the indicated RNAs in LLIs (n= 53) versus controls (n= 65). None of the differences reached statistical significance, after adjustment for sex distribution.